One-week glucose control via zero-order release kinetics from an injectable depot of glucagon-like peptide-1 fused to a thermosensitive biopolymer

Kelli M. Luginbuhl[1], Jeffrey L. Schaal[1], Bret Umstead[2], Eric M. Mastria[1], Xinghai Li[1], Samagya Banskota[1], Susan Arnold[2], Mark Feinglos[3], David D'Alessio[3] and Ashutosh Chilkoti[1]*

Stimulation of the glucagon-like peptide-1 (GLP1) receptor is a useful treatment strategy for type 2 diabetes due to pleiotropic effects, such as the regulation of islet hormones and the induction of satiety. However, the native ligand for the GLP1 receptor has a short half-life owing to enzymatic inactivation and rapid clearance. Here, we show that a subcutaneous depot formed after a single injection of GLP1 recombinantly fused to a thermosensitive elastin-like polypeptide results in zero-order release kinetics and circulation times of up to 10 days in mice and 17 days in monkeys. The optimized pharmacokinetics lead to 10 days of glycaemic control in three different mouse models of diabetes, as well as the reduction of glycosylated haemoglobin levels and weight gain in ob/ob mice treated once weekly for 8 weeks. Our results suggest that the optimized GLP1 formulation could enhance therapeutic outcomes by eliminating peak-and-valley pharmacokinetics and improving overall safety and tolerability. The design principles that we established should be broadly applicable for improving the pharmacological performance of other peptide and protein therapeutics.

Nearly 30 million adults in the United States are diabetic, with over 1.7 million new cases diagnosed in 2012. It is estimated that diabetes causes $176 billion direct medical costs annually, and there were over 455,000 emergency room visits due to diabetes-related glycaemic crises in 2011[1]. These statistics highlight the staggering burden of this disease on the healthcare system. Of those afflicted, over 90% of adult diabetes cases are type 2. Yet, despite the long list of treatment options among a growing number of drug classes, nearly half of diagnosed type 2 cases are not properly managed[2]. These patients routinely fail to reach established glycaemic targets, due largely to the tapering efficacy of monotherapies over time, and inadequate patient adherence to prescribed treatment regimens, which often require frequent and complicated meal-specific dosing. Furthermore, many of the most widely prescribed medications are plagued by undesirable side effects, including weight gain and a risk of hypoglycemia[3].

Glucagon-like peptide-1 (GLP1) receptor agonists are a class of recently developed diabetes drugs with the therapeutic potential to address all of these treatment challenges. The parent peptide, GLP1, is a 31-amino-acid incretin hormone derived from post-translational processing of the proglucagon gene[4,5]. It is secreted from L cells in the lower intestine and colon postprandially[6]. In addition to stimulating insulin secretion, GLP1 has been shown to: (1) induce satiety[7]; (2) mediate weight loss[8]; and (3) prevent apoptosis and enhance proliferation of pancreatic β cells[9], which can help to slow disease progression.

Diabetes is a chronic disease whose treatment is complicated by constantly changing insulin demands based on an intricate balance of diet, metabolism and activity. Therefore, the treatment of diabetes poses a unique drug delivery challenge. GLP1 is an attractive drug for treatment for type 2 diabetes due to its glucose-dependent mechanism of action—it only stimulates a strong insulin response when glucose levels reach a threshold concentration[10,11]. Thus, maintaining high levels of GLP1 by constant intravenous (IV) infusion is very effective for promoting insulin secretion in diabetic subjects when glucose levels are elevated[12–14], which normalizes both fasting[15] and postprandial[13] blood glucose without incidence of hypoglycaemia. Unfortunately, the clinical utility of GLP1 is limited by its short two-minute half-life[16], owing to its small size, rapid clearance by renal filtration, and inactivation by the ubiquitous cell-surface exopeptidase DPP-IV[17].

There is a large body of literature focused on extending the half-life of GLP1, to enhance its therapeutic potential[18] as well as patient convenience and compliance. Drugs that promote GLP1 receptor signalling have been successfully developed for the treatment of diabetes[19]; they have meaningfully impacted clinical practice and are widely used. Albiglutide (Tanzeum) and dulaglutide (Trulicity) are once-weekly GLP1 formulations recently approved for use in patients with type 2 diabetes that achieve long half-lives through fusion with protein partners that have slow turnover rates—albumin and an engineered Fc fragment, respectively.[18] By extending GLP1's half-life to 3–7 days in humans[20,21], these drugs are able to reduce the required dose and dosing frequency. Both have been FDA approved for once-weekly administration via subcutaneous (SC) injection. However, the strategies to continue improving GLP1 pharmacokinetics through recombinant engineering and reduced renal clearance are approaching an asymptote. Because improvements in circulating half-life have reached a limit, the duration of these treatments can only be further modulated by an increase in dose, which is ultimately constrained by the therapeutic window, toxicity and cost.

To further advance the field of GLP1 therapy, next-generation formulations must also prioritize mechanisms that control release.

[1]Department of Biomedical Engineering, Duke University, Durham, North Carolina 27708, USA. [2]PhaseBio Pharmaceuticals, Inc., Malvern, Pennsylvania 19355, USA. [3]Division of Endocrinology, Metabolism, and Nutrition, Duke University Medical Center, Durham, North Carolina 27710, USA.
*e-mail: chilkoti@duke.edu

Significant improvements to control GLP1 receptor agonist release have been achieved using injectable synthetic polymer formulations. For example, tri-block copolymers mixed with a GLP1 receptor agonist form a gel *in situ*, encapsulating the drug and controlling its release to achieve 7–10 days of glucose control in mice[22,23]. However, synthetic polymer formulations can require multi-component mixtures of polymer, drug and excipients, and can raise concerns regarding buildup of the gel's degradation products. Currently, Bydureon is the only FDA-approved controlled release formulation on the market, using poly-lactic-co-glycolic acid (PLGA) microsphere technology to encapsulate and sustain the release of a GLP1 analogue, exenatide.[24,25] This formulation is also approved for once-weekly administration, but is not without its own limitations such as poor shelf-life stability, burst release and injection discomfort—the 0.06-mm-diameter microspheres require larger needles for SC injection.[26,27] Thus the GLP1 receptor agonist field still has a need for new sustained-release therapies that can achieve steady therapeutic levels of a drug in circulation. This drug release profile, termed zero order kinetics, is ideal for both reducing dosing frequency and minimizing classic peak and valley pharmacokinetics. Such a formulation would be likely to reduce gastrointestinal side effects, improve patient comfort, and further dissociate compliance from therapeutic outcome.

Towards this goal, we have coupled half-life extension with a controlled release system by fusing GLP1 to a thermally sensitive biopolymer, elastin-like polypeptide (ELP). ELPs are a class of recombinant polymer that enhance the pharmacokinetics and bioavailability of the therapeutic proteins to which they are fused[28]. They are large, intrinsically disordered, random-coil polypeptides comprised of a repeated Val-Pro-Gly-Xaa-Gly (VPGXG) pentapeptide monomer, a motif derived from human tropoelastin. ELPs are genetically encoded and synthesized in *Escherichia coli*, providing high yields of monodisperse biopolymer that are stimuli-responsive, biocompatible and biodegradable.[29] They also exhibit lower critical solution temperature (LCST) phase transition behaviour[30], which enables them to rapidly transition from a soluble state to an insoluble coacervate with the addition of heat or salt. This phase transition is reversible following dilution such that, in response to the concentration decay at the boundary layer of the depot, the transitioned ELP slowly dissolves from the margins into the core, releasing ELP–drug fusions at a steady rate. This feature of ELPs distinguishes them from other polypeptides and synthetic polymers, and makes them an attractive technology for addressing the challenges of peptide drug delivery. The phase transition temperature (T_t) can be tuned by adjusting the molecular weight (M_w) (number of VPGXG repeats) or hydrophobicity (X guest residue composition). The T_t can be precisely engineered such that the fusion remains soluble in a syringe at room temperature, but transitions to an insoluble, slow-releasing coacervate when injected, triggered by the increase from ambient to body temperature.

We previously reported proof of principle of a GLP1–ELP fusion, where a single SC injection of first-generation GLP1–ELP combined sequence modification of GLP1 for degradation resistance (see Methods) and prolonged circulation with sustained release to achieve 5 days of glucose control in healthy C57Bl/6J mice[31], but only 2–3 d in ob/ob or db/db mice[32]. Herein, we systematically investigate the impact of molecular design features on the temporal duration of drug release. In this study, we chose to independently optimize the two most important and orthogonal molecular parameters: the ELP M_w and the fusion T_t, both of which can be tuned at the gene level. By optimizing the M_w and T_t of the GLP1–ELP fusion, we achieve sustained release of the GLP1–ELP fusion after a single SC injection and can control glucose for up to 10 days in three different and challenging diabetic mouse models. To our knowledge, this is the longest duration of glucose control reported for any recombinant GLP1 fusion system. We also characterized the

pharmacokinetics of the depot in mouse and monkey models to assess clinical viability in humans. The 17 days of sustained release in monkeys achieved with our GLP1–ELP fusion is superior to two molecularly engineered formulations of GLP1—Tanzeum and Trulicity—in comparable rodent and non-human primate studies. These two GLP1 receptor agonists are clinically approved for once-weekly administration, suggesting that our optimized GLP1–ELP fusion may provide the first once-monthly formulation of GLP1 in humans.

Results

Optimal T_t for controlling GLP1–ELP release. We hypothesized that GLP1–ELP fusions with T_t further below body temperature would form a more stable depot capable of slow, sustained release. To test this hypothesis, we designed and recombinantly expressed a set of GLP1–ELP fusions with T_t values that span 15 to 36 °C, remaining at or below the SC temperature of wild-type C57Bl/6J mice[33]. A non-depot-forming control, transitioning well above body temperature at 49 °C, was also constructed. The number of VPGXG pentapeptides was kept constant at 120 repeats for all constructs, while the amino acid composition of the X guest residue motif was adjusted to modulate the T_t (which is reflective of the degree of hydrophobicity of the guest residue composition). We constrained our design by filling the guest residue with only three amino acids—Ala, Val and Leu— in order to minimize differences in M_w and reduce any intrinsic molecular differences between the ELP aggregates. All constructs were synthesized in *E. coli* and purified to greater than 95% purity, as assessed using sodium dodecyl sulfate (SDS)–polyacrylamide gel electrophoresis (SDS–PAGE) (Supplementary Fig. 6a). Each construct's composition, phase transition behaviour, hydrodynamic radius (R_h) and *in vitro* activity are summarized in Table 1.

As guest residue hydrophobicity was increased, the T_t of the GLP1–ELP fusion was depressed (Fig. 1a) and its concentration dependence was reduced (Fig. 1b). The subscript in each fusion's nomenclature represents its T_t in °C at the injected concentration used for *in vivo* studies, which is indicated by the dotted outline in Fig. 1b. Regardless of T_t, all constructs retained reversible phase behaviour (Fig. 1a). Fusion of GLP1 to an ELP reduced its potency by approximately 5- to 40-fold compared with native GLP1 peptide (Fig. 1c), whose measured half-maximal effective concentration (EC$_{50}$) of 0.7 nM (0.5 to 1.0 nM 95% confidence interval, CI) is in agreement with values reported from similar studies[34,35]. This finding was not surprising, given that fusion of GLP1 to albumin results in a 30-fold reduction in bioactivity[36]. This was also better than conjugation of GLP1 to PEG, which reduced receptor affinity by 30- to 500-fold[37]. Although there is a trend towards reduced potency for fusions with lower T_t values, this trend is not significant and was probably due to their greater propensity to transition and aggregate at the assay temperature (37 °C); such aggregation could sterically hinder interaction with the GLP1 receptor. For example, GLP1–ELP$_{15.5}$ and GLP1–ELP$_{21.4}$ are estimated to undergo a 37 °C phase transition at concentrations of 5 pM and 40 nM, respectively, and therefore are likely to exist as insoluble aggregates at some of the concentrations tested in the bioassay.

We next examined the *in vivo* efficacy of this series of constructs with variable T_t, but a near-constant M_w of ~50 kDa. All constructs were kept on ice to ensure solubility prior to SC injection into the scruff of the neck of 7-week-old diet-induced obese (DIO) mice. Mice were treated with 700 nmol kg^{-1} GLP1–ELP at 500 μM or an equivalent volume of phosphate-buffered saline (PBS). Blood glucose was measured 24 h before and immediately prior to injection. After treatment, it was monitored periodically throughout the first day (Supplementary Fig. 8), and then every 24 h thereafter (Fig. 1d). Body weight response to treatment was similarly tracked

Table 1 | Summary of GLP1–ELP fusions and their characterization.

| Construct name	Xaa composition (Ala:Val:Leu)	VPGXG repeats (N)	T_t at injected conc. (°C)	M_w (kDa)	R_h (nm)	In vitro EC_{50} (nM)	In vitro EC_{50} 95% CI (nM)
T_t series (subscript: temp. in °C)							
GLP1–ELP$_{15.5}$	0:6:4	120	15.5	53,446	5.3 ± 0.1	26.0	14.4 to 47.0
GLP1–ELP$_{21.4}$	0:1:0	120	21.4	52,772	6.2 ± 0.1	13.0	7.5 to 22.4
GLP1–ELP$_{30.2}$	5:5:0	120	30.2	51,209	6.0 ± 0.1	7.1	2.9 to 17.3
GLP1–ELP$_{35.5}$	6:5:0	120	35.5	50,873	6.3 ± 0.1	3.8	2.2 to 6.4
GLP1–ELP$_{48.8}$	9:1:0	120	48.8	49,742	5.9 ± 0.1	6.6	4.4 to 9.9
M_w series (subscript: M_w in kDa)							
GLP1–ELP$_{20.0}$	0:1:0	40	31.5	20,013	4.4 ± 0.1	12.5	6.4 to 24.3
GLP1–ELP$_{35.8}$	3:7:0	80	29.9	35,840	5.3 ± 0.1	5.7	1.8 to 17.7
GLP1–ELP$_{67.5}$	4:6:0	160	30.6	67,476	7.4 ± 0.1	11.8	5.1 to 27.2
GLP1–ELP$_{98.7}$	5:5:0	240	32.3	98,664	8.0 ± 0.3	10.1	6.2 to 16.4
μSPECT-CT samples							
GLP1–ELP$_{opt}$	4:6:0	160	30.6	67,476	7.4 ± 0.1	11.8	5.1 to 27.2
GLP1–ELP$_{sol}$	1:0:0	160	54.6	64,783	7.4 ± 0.1	11.0	5.0 to 24.0
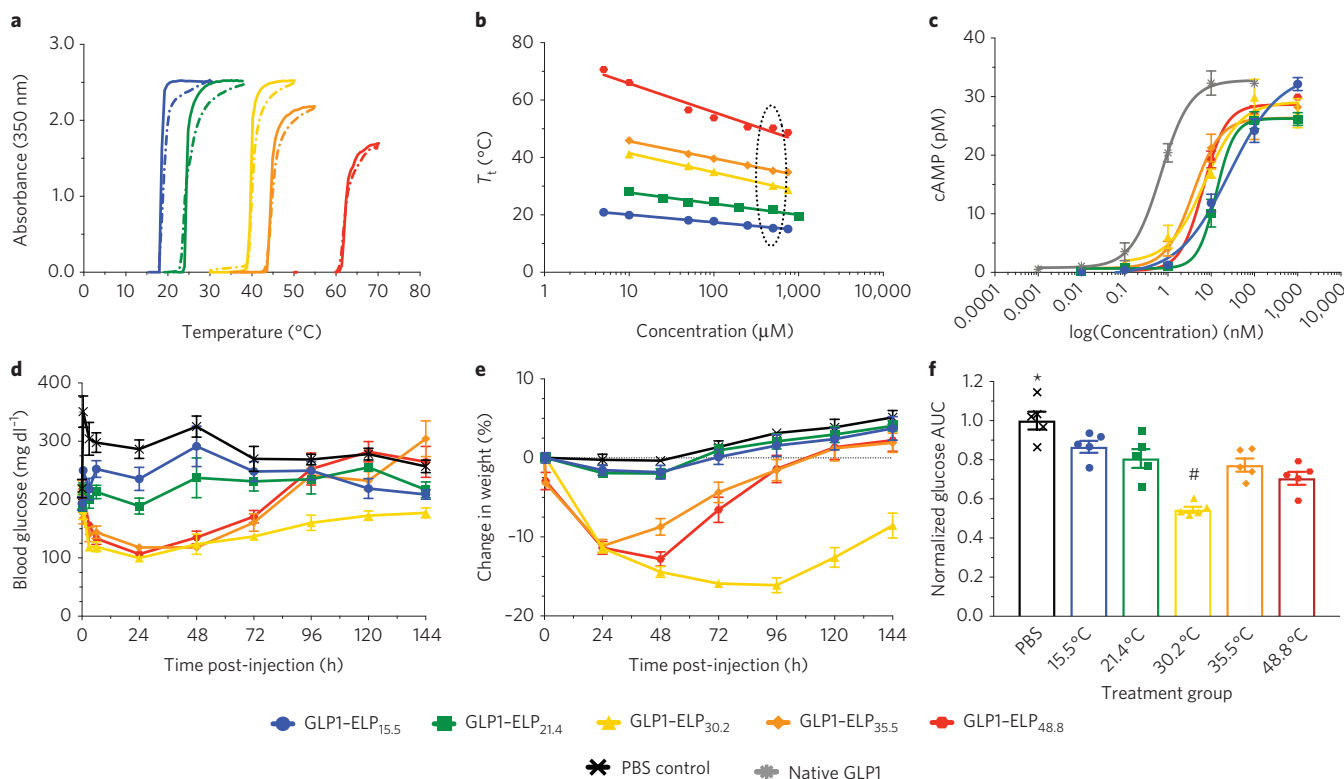
Figure 1 | A set of GLP1–ELP fusions with constant number of repeats but varied T_t was characterized and tested in vivo. a,b, Optical density was monitored during heating (solid) and cooling (dashed) to demonstrate reversible phase behaviour (data shown for constructs at 50 μM, $n = 1$) (**a**) and to determine the concentration dependence of T_t (**b**), where the dotted oval indicates the varied T_t values at the injected concentration in vivo. **c**, Activity was assayed in vitro by measuring cAMP response ($n = 3$) after receptor stimulation with fusions or native GLP1 control. **d,e**, Blood glucose (**d**) and percent weight change relative to weight at $t = 0$ (**e**) were monitored after treating seven-week-old DIO mice ($n = 5$) with a single SC injection of GLP1–ELP fusions or PBS control. **f**, 144 h AUC was quantified for each subject and normalized to the PBS controls to compare glycaemic regulation across treatment groups. * and # indicate groups that are statistically significantly different ($P < 0.05$) from all other groups. Data represent the mean and s.e.m. Subscript numbers in GLP1–ELP nomenclature in the key are T_t (°C).

(Fig. 1e). Glucose area under the curve (AUC) for the duration of the experiment (144 h) was determined for all treatment groups by integrating blood glucose over time and normalizing these values to the PBS control group (Fig. 1f). All treatment groups had a significantly lower glucose AUC than the PBS control group ($P < 0.05$, ANOVA and Dunnett's Test). The constructs with higher T_t values (GLP1–ELP$_{35.5}$ and GLP1–ELP$_{48.8}$) had a bolus-type release, with quick absorption followed by a rapid decline in efficacy.

In contrast, the more hydrophobic constructs (GLP1–ELP$_{15.5}$ and GLP1–ELP$_{21.4}$) released less drug and achieve only modest reductions in glucose and weight. Of the designs tested, the fusion with a T_t of 30.2 °C, just below the SC temperature of mice[33], significantly outperformed all other GLP1–ELP constructs in both magnitude and duration of effect, controlling blood glucose and effecting weight loss for 6 days.

The M_w threshold above which GLP1–ELP fusions perform best. Having identified an optimal T_t for GLP1–ELP depot efficacy, we next asked if M_w also altered the performance of GLP1–ELP. To test the effects of this genetically tunable variable, we constructed a second set of GLP1–ELP fusions with reversible phase behaviour (Fig. 2a) that spanned a wide range of M_w, but that all exhibited the same optimal T_t of approximately 30 °C (indicated by the dotted outline in Fig. 2b). This was achieved by manipulating the X guest residue ratio in the ELP, such that larger fusions had a greater proportion of the hydrophilic amino acid Ala and smaller fusions had a greater percentage of the hydrophobic amino acid Val. A predictive model developed previously[38] was used to minimize the iterative design, synthesis and characterization process needed to build the final set of fusions. These fusions were constructed to span a specific range of M_w with two parameters in mind: (1) the renal filtration cutoff size for globular proteins (50–70 kDa)[39,40] and (2) the polymer sizes at which PEGylated proteins show an abrupt reduction in renal clearance (30 kDa)[41–43]. The subscript in each fusion's nomenclature represents its M_w in kDa.

The purity of these constructs was analysed using SDS–PAGE (Supplementary Fig. 6b). Their sizes were measured by dynamic light scattering (DLS) and the reversible phase behaviour was confirmed (Fig. 2a). While the 20.0 kDa fusion has an R_h of only 3.5 nm, the 98.7 kDa construct has an R_h greater than 8 nm. These values correlate well with data reported for dextrans and linear PEG[44] (Supplementary Fig. 7), which is reasonable considering ELP and PEG share many similarities—both are random, unstructured and well-hydrated polymers. There was no statistically significant correlation between *in vitro* activity and M_w (Fig. 2c). However, as was seen with the first set of GLP1–ELP fusions, the overall EC$_{50}$ of fusions is increased by approximately 10–20-fold compared to native GLP1. Full characterization of this set of fusions can be found in Table 1.

By increasing the number of VPGXG repeats and, thus, the fusion M_w, the concentration dependence of T_t decreases; all of the T_t values of these fusions have a slightly different concentration dependence, as indicated by the variable slopes of their T_t versus log(concentration) plots (Fig. 2b). Importantly, all the plots intersect at a concentration of ~200 μM, with a T_t of 29.4–32.1 °C. This concentration, at which the T_t is nearly constant across constructs, was chosen for *in vivo* efficacy studies. This set of fusions was used to treat 7-week-old DIO mice. Mice received a SC depot injection (700 nmol kg^{-1} at 200 μM) and negative control animals were injected with an equivalent volume of saline. Glucose and weight were measured prior to injection and glucose was monitored
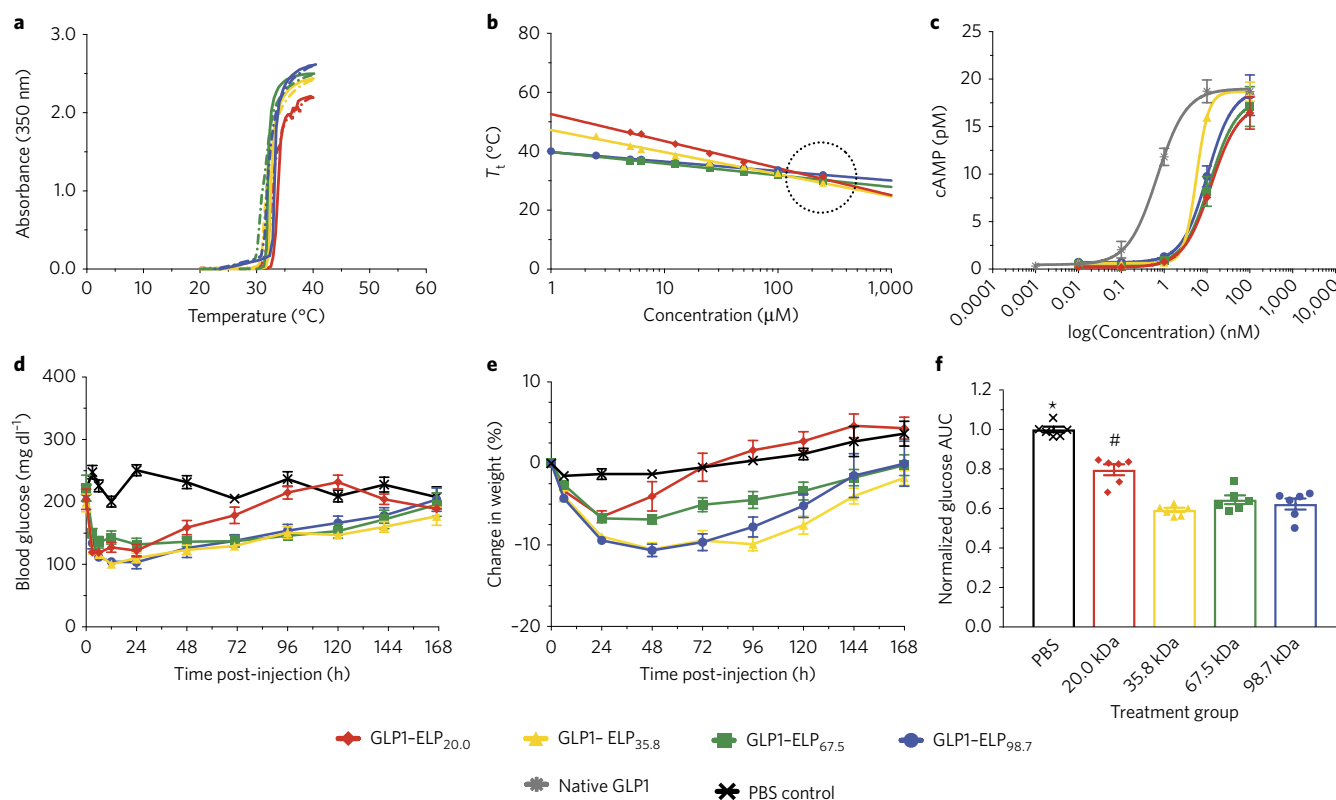

Figure 2 | A set of GLP1–ELP fusions with constant T_t at the injected concentration but varied M_w was characterized and tested *in vivo*. a,b, Optical density was monitored during heating (solid) and cooling (dashed) to demonstrate reversible phase behaviour (data shown for constructs at 100 μM, $n = 1$) (**a**) and to confirm that the T_t for all constructs remains constant at the injected concentration, indicated by the dotted circle (**b**). **c,** Activity was assayed *in vitro* by measuring cAMP response ($n = 3$) after receptor stimulation with fusions or native GLP1 control. **d,e,** Blood glucose (**d**) and percent weight change relative to weight at $t = 0$ (**e**) were monitored after treating 7-week-old DIO mice ($n = 6$) with a single SC injection of GLP1–ELP fusions or PBS control. **f,** 144 h AUC was quantified for each subject and normalized to the PBS controls to compare glycemic regulation across treatment groups. * and # indicate groups that are statistically significantly different ($P < 0.05$) from all other groups. Data represent the mean and s.e.m. Subscript numbers in GLP1–ELP nomenclature in the key are M_w (kDa).

periodically throughout the first day (Supplementary Fig. 9a) and then every 24 hours until effects were no longer observed (Fig. 2d,e). Glucose AUC for the duration of observed efficacy (144 h) was determined for all treatment groups and normalized to the PBS control group (Fig. 2f).

The 144 h AUC values for all treated groups were significantly lower than the PBS control group ($P < 0.05$, ANOVA and Dunnett's Test). Additionally, the AUC for the mice treated with the 20.0 kDa fusion was significantly different from all other treatment groups ($P < 0.05$). Unsurprisingly, this data indicated that the glomerular filtration dependence of GLP1–ELP fusions more closely resembles that of linear polymers such as PEG rather than globular proteins such as albumin (Supplementary Fig. 7). This data suggests that the 20.0 kDa fusion, whose 4.4 nm R_h was most similar to the 3.6 nm size of human serum albumin[45], is below the kidney filtration cutoff, while the other constructs with a M_w of 35.8 kDa or greater have prolonged circulation times due to their larger size and reduced filtration. This hypothesis was further confirmed when constructs were IV injected (Supplementary Fig. 9b) after dilution to 1 µM to prevent the phase transition from occurring; the T_t for all constructs at this concentration is above 37 °C. Glucose-lowering effects of the smallest construct (20 kDa) manifested most quickly, but diminished rapidly and were no longer apparent by 12 h post-injection, while all other constructs maintained more steady reductions in blood glucose that lasted beyond 12 h. This data is in good agreement with literature where PEG has been shown to have a sharp increase in half-life at 30 kDa[43].

Optimized GLP1–ELP fusion is suitable for once-weekly injection in three mouse models of diabetes. Having optimized the T_t and M_w, we selected the optimal 67.5 kDa GLP1–ELP—subsequently referred to as GLP1–ELP$_{opt}$—for future efficacy studies. This construct was selected because it had an optimal T_t as well as the highest expression in *E. coli* and the least apparent burst release, indicated by a sharper dip in blood glucose and weight loss in the first few days of treatment (Fig. 2e and Supplementary Fig 9a). Upon completing a dose-response experiment, which verified that 700 nmol kg^{-1} was the optimal dose (Supplementary Fig. 10a–c), we tested this construct's efficacy in three models of diabetes with varying degrees of severity: C57Bl/6J mice maintained on a high-fat diet for 11 weeks (Fig. 3a–c), ob/ob mice with a mutant leptin gene (Fig. 3d–f), and db/db mice with a mutant leptin receptor gene (Fig. 3g–i). All mice received a single SC injection of either 700 nmol kg^{-1} GLP1–ELP$_{opt}$ or an equivalent volume of saline. Blood glucose and body weight were monitored for 10 days post-treatment, and 240 h blood glucose AUC was quantified and normalized to the PBS control group.

Treatment with the optimal depot-forming GLP1–ELP fusion significantly reduced total glucose exposure (glucose AUC) by 50% or more in all three models ($P < 0.05$, Student's *t*-test). In both the DIO and ob/ob models, mice treated with GLP1–ELP$_{opt}$ lost weight while PBS-treated control mice gained weight (Fig. 3b,e). There was no effect of treatment on weight in the most severely diabetic db/db model (Fig. 3h). This treatment also regulated blood glucose for up to 10 days in all three mouse models (Fig 3a,d,g). In contrast, the first-generation GLP1–ELP fusion showed only 3 days of control in ob/ob mice[32]. The immediately apparent and important consequence of this optimization exercise is the substantial increase in the duration of controlled release, doubling glucose control from 5 days in healthy mice[31] to 10 days in three far more challenging diabetes models after a single injection.

To further validate the robustness of this delivery system, we performed an intraperitoneal glucose tolerance test (IPGTT) at days 3 and 6 post-injection in the ob/ob strain to quantify how treatment alters the ability to respond to a glucose challenge (Fig. 3j–l). The effect of treatment on IPGTT AUC was significant ($P < 0.05$, two-way ANOVA); however, there was neither a

significant effect of time post-treatment nor an interaction term between treatment and time. The data suggest that the extent of response to a glucose challenge on day 3 (Fig. 3j) was not statistically different from that on day 6 (Fig. 3k), which is an indication that our GLP1–ELP system maintained its ability to dynamically regulate glycaemic control over the course of a week. The difference in AUC between the treatment and control group was significant ($P < 0.05$, Bonferroni multiple comparison test) at both time points (Fig. 3l).

In a separate study, we performed histology at the site of injection in male ob/ob mice treated bilaterally with GLP1–ELP$_{opt}$, PBS or PLGA microspheres ($n = 3$). Five days after treatment, the injection site was dissected, fixed, paraffin embedded, cut into 5 µm sections, and stained with haematoxylin and eosin (H&E) (Supplementary Fig. 14). The slides were imaged and analysed by a pathologist who was blinded to the group assignments. No concerning inflammation, irritation or dermal thickening was observed in the GLP1–ELP$_{opt}$ slides. In contrast, mild histiocytic inflammation—consistent with the timing of 5 days post-injection of foreign material—was seen in all PLGA-treated samples, but in only one GLP1–ELP$_{opt}$ treated sample. Full histopathological analysis of the sections can be found in Supplementary Section 3.6.

Fusion of GLP1 to a depot-forming ELP yields favourable zero-order release kinetics and improved pharmacokinetic properties in mice. Having seen significant efficacy in three different mouse models of diabetes, we next investigated the depot's release kinetics and pharmacokinetics to better understand how our results might translate into humans. Using modified free peptide (GLP1) and GLP1 fused to a soluble ELP (GLP1–ELP$_{sol}$) as controls, we performed a single SC injection in ob/ob mice ($n = 4$) with radiolabelled constructs. ^{125}I was selected for its long half-life and because it enabled us to simultaneously collect blood for pharmacokinetic analysis and image the SC depots with micro-single photon emission computed tomography with X-ray computed tomography (µSPECT-CT). Anatomically registered µSPECT-CT images were used to quantify depot retention with time by analysing the region of interest (ROI) containing the depots, and excluding the pancreas, thyroid and bladder.

A separate cohort of mice was IV injected with 10 nmol kg^{-1} radiolabelled construct to determine the elimination half-life ($T_{1/2\text{-elim}}$), clearance (CL), volume of distribution (V_d) and bioavailability (F). For IV injection, the constructs were diluted to 1 µM, a concentration low enough to prevent the fusions from transitioning in circulation. Counts per minute (CPM) in blood samples, measured using a gamma counter, were converted to concentration for calculation of pharmacokinetic parameters, which is explained in detail in the Methods section. Table 2 summarizes these parameters for each of the three constructs—free peptide, GLP1–ELP$_{sol}$ and GLP1–ELP$_{opt}$. $T_{1/2\text{-elim}}$ is defined as the time it takes to decrease the plasma concentration of a drug by half, whereas the apparent, or biological, half-life ($T_{1/2\text{-biol}}$) accounts for drugs whose rate of plasma concentration decline is dependent on other factors, such as route of administration, rate of absorption or controlled release.

Fusion to an ELP increased the peptide's elimination half-life from 5 min to approximately 6 h for both the soluble and depot-forming GLP1–ELP constructs. In contrast, with SC injection, fusion to a depot-forming ELP provided a 10-fold improvement in $T_{1/2\text{-biol}}$ of GLP1, increasing it to 45.2 h compared to 4.7 h for the GLP1 peptide alone. As expected, fusion to an ELP extended the time it took to reach peak concentration (t_{max}) by 8-fold. The depot-forming ELP also prevented burst release, as evidenced by the 10-fold lower C$_{max}$ value, despite the fact that both fusions were administered at the same dose. This reduced burst release is advantageous as it prevents wasted drug, better maintains plasma drug concentration within the therapeutic window, and minimizes side effects. This minimization in burst release is also reflected in
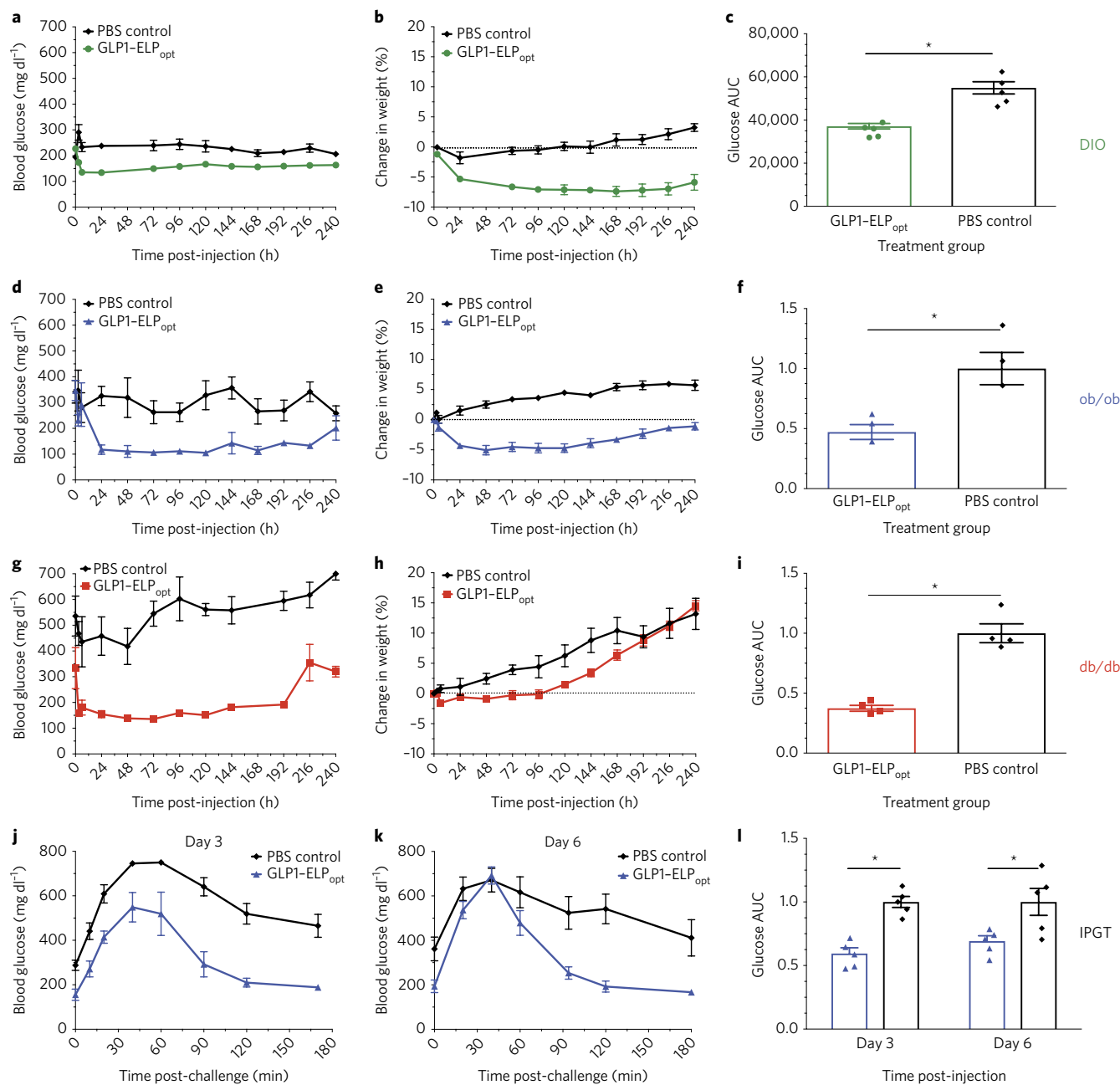
Figure 3 | GLP1–ELP fusions were effective at controlling blood glucose levels for up to 10 days in three murine models of diabetes. a–i, Blood glucose and percent weight change were monitored over 10 d after a single injection of either GLP1-ELP$_{opt}$ or an equivalent volume of PBS in DIO mice ($n = 5$) (**a,b**), ob/ob mice ($n = 3$) (**d,e**) and db/db mice ($n = 4$) (**g,h**). Blood glucose AUC was calculated over 240 h and normalized within each experiment (by strain) to the PBS control group (**c,f,i**). **j,k**, In the male ob/ob model ($n = 5$), after a single injection, treated mice had an improved response to a 1 g kg^{-1} glucose challenge compared with PBS controls on days 3 (**j**) and 6 (**k**) post-injection. **l**, The normalized blood glucose AUC over 180 min is statistically significant at both day 3 and day 6. *$P < 0.05$. Data represent the mean and s.e.m.

drug AUC. GLP1–ELP$_{opt}$ had half the total overall exposure compared to GLP1–ELP$_{sol}$, yet, despite this, was able to regulate blood glucose for a week longer.

CL, a measure of the plasma volume cleared of drug per unit time, showed a much larger value for the peptide, which is freely filtered by the kidneys. The CL values for both GLP1–ELP$_{sol}$ and GLP1–ELP$_{opt}$ again highlight the pharmacological benefit of fusion to an ELP, which reduced renal filtration and slowed clearance of the drug, extending its duration of efficacy. Bioavailability, a measure of the amount of drug that is able to reach circulation and exert its effect, was nearly 100% for the free GLP1 and about 3-fold lower for the

fusions. We consider this an acceptable tradeoff given the remarkable improvements in pharmacokinetics. Furthermore, image quantification on day 10 proved that approximately 18% of the depot remains at the injection site (Fig. 4a). Thus, the calculated bioavailability of GLP1–ELP$_{opt}$ is likely to be a low approximation because the study was terminated before the depot was fully expended.

Using µSPECT-CT, the radiolabelled depot-forming GLP1–ELP$_{opt}$ is visible in the SC space on day 10, whereas the free peptide and soluble controls are absorbed into circulation by 24 h (Fig. 4a). Depot retention, normalized for each subject to total image intensity at time 0 h, quantitatively confirms the controlled release capabilities

Table 2 | Summary of the pharmacokinetic properties of GLP1 and GLP1–ELP fusions.

Construct	$T_{1/2\text{-elim}}$ (h)*	$T_{1/2\text{-biol}}$ (h)*	t_{max} (h)	C_{max} (nM)	Delivery duration (d)	AUC (nM×h)	CL (ml h^{-1})	Bioavailability (%)
GLP1	0.08 (0.06 to 0.12)	4.7 (3.4 to 7.0)	0.75	$484 \pm 26^\dagger$	< 1	$4,418 \pm 618^\dagger$	2.88 ± 0.48	98.1 ± 22.8
GLP1–ELP$_{sol}$	5.7 (3.8 to 11.4)	16.9 (14.5 to 20.3)	6	$2,123 \pm 49$	3	$56,451 \pm 1,782$	0.23 ± 0.01	38.6 ± 0.8
GLP1–ELP$_{opt}$	6.9 (5.3 to 9.8)	45.2 (33.7 to 68.3)	6	295 ± 13	10	$29,872 \pm 1,069$	0.42 ± 0.10	33.4 ± 21.0

*Values reported are the mean with 95% CI range in parentheses. $^\dagger C_{max}$ and AUC for GLP1 are lower than the values for GLP1–ELP because of the lower treatment dose used for free peptide (50 nmol kg^{-1}) versus GLP1–ELP fusion (700 nmol kg^{-1}).

of GLP1–ELP$_{opt}$ for over a week (Fig. 4b). When an exponential decay line—$y_t = (y_0 - b)e^{-kt} + b$—is fit to the percent retention data (Fig. 4b), the first-order rate constants are 0.14 ± 0.06 h^{-1} ($R^2 = 0.99$) and 0.01 ± 0.01 h^{-1} ($R^2 = 0.87$) for GLP1–ELP$_{sol}$ and GLP1–ELP$_{dep}$, respectively. The depot's first-order rate constant is very small, indicative of slower decay that can be approximated as a zero-order rate constant. When fit to a linear model, the zero-order rate constant was found to be 0.25 ± 0.04 %$_{ret}$ h^{-1} with an $R^2 = 0.84$, almost equal to the goodness-of-fit value obtained from the exponential decay model. To further support our observation of near zero-order release kinetics, the cumulative AUC of drug in circulation was plotted against time (Fig. 4c). This plot shows steady, linear release of GLP1–ELP$_{opt}$ compared to GLP1–ELP$_{sol}$ and free GLP1, which follow a logarithmic release profile. Biodistribution of mice treated with GLP1–ELP$_{opt}$ on day 10 revealed that the highest levels of drug remained at the injection site and thyroid (due to radiolabelled iodine uptake) with no remarkable accumulation in other organs, including the kidneys and liver (Supplementary Fig. 11). Pharmacodynamics in the same mouse model indicate that whatever GLP1–ELP$_{opt}$ was still releasing beyond this time point was below the theoretical minimum effective concentration (Fig. 4d) because blood glucose levels were only modestly lower than PBS-treated controls (Supplementary Fig. 12). A full panel of all µSPECT-CT images can be found in Supplementary Fig. 13.

Optimized GLP1–ELP depots have long-term efficacy in mice.
To ensure the long-term efficacy of our optimized depots, we SC injected ob/ob mice once-weekly with 700 mol kg^{-1} of GLP1–ELP$_{opt}$. Glucose and weight were monitored regularly. Prior to the initial injection and after 4 and 8 weeks of treatment, the percentage of glycosylated haemoglobin (%HbA1c) was measured using a Siemens DCA Vantage Analyzer, which uses an immunoassay platform. The average %HbA1c level in lean, untreated male C57Bl/6J mice is reported to be 4.0%[46]. %HbA1c levels are useful in diabetes management because they provide an integrated view of glycaemia over an extended period of time—changing only as red blood cells (RBCs) turn over—and are less sensitive to daily fluctuations due to eating and activity. While it is recommended that patients have their %HbA1c checked every 3–4 months, we selected an 8-week treatment period because the lifespan of RBCs in mice is shorter than in humans ($T_{1/2} \approx 40$–60 d in rodents[47] versus 120 d in humans[48]).

Prior to starting treatment at day 0, 5-week-old male ob/ob mice in both the GLP1–ELP$_{opt}$ and PBS control groups ($n = 5$) had identical %HbA1c levels of about 4.4 (Table 3). By day 28, the treated group had significantly lower %HbA1c than control mice ($P < 0.05$, Student's t-test). At day 56, although %HbA1c continued to rise in both the treated and control groups, the difference in %HbA1c was equally pronounced ($P < 0.05$, Student's t-test). When each animal's 28- and 56-day %HbA1c values were plotted against their corresponding glucose AUC, there is a correlation ($R^2 = 0.66$, $P < 0.05$) and the linear fit predicts a y-intercept of 4.4, the mean %HbA1c at day 0 (Supplementary Fig. 15a). The treatment regimen with GLP1–ELP$_{opt}$ successfully reduced overall glucose exposure by more

than 32% ($P < 0.05$, Student's t-test). While treatment did not affect weight loss, mice in the GLP1–ELP$_{opt}$ group gained an average of 20% less weight than PBS-treated controls and had a lower mean weight at the conclusion of the study ($P < 0.05$, Student's t-test). These results are summarized in Table 3. Long-term efficacy in male DIO mice was also investigated over a 56-day period, showing significant reduction in %HbA1c between treated and control mice (Table 3) with correlation to mean glucose (Supplementary Fig. 15b). The 8-week treatment significantly reduced total glucose AUC ($P < 0.05$, Student's t-test) and was more successful in this model at slowing weight gain.

GLP1–ELP depots persist for two weeks in non-human primates.
Because they have a much faster metabolism, mice typically clear a drug more quickly than humans and other larger animals. Thus, on the basis of allometry[49], we expected our optimized fusion to last longer in monkeys than in mice. Towards the goal of a bi- or once-monthly injectable treatment option for diabetes patients, we next investigated the pharmacokinetics of the optimized fusion in non-human primates. Fusion-protein-naive male cynomolgus macaque monkeys received a single SC injection at a dose of 150 nmol kg^{-1} GLP1–ELP$_{opt}$ ($n = 3$). The GLP1–ELP$_{opt}$ sample for *in vivo* testing in monkeys was expressed and purified by PhaseBio Pharmaceuticals (Malvern); details can be found in Supplementary Section 1.4.

Pharmacokinetics of the circulating GLP1–ELP$_{opt}$ fusion released from a SC depot was quantified using a sandwich ELISA with anti-GLP1 and anti-ELP antibodies (detection limit = 2.44 ng ml^{-1}). Mean plasma levels of GLP1–ELP$_{opt}$ remained nearly constant until day 10 (Fig. 5a). The drug was detectable in all three subjects until 17 d and, in subject 2, up to 21 d (Fig. 5b). Blood glucose was monitored at the time of blood draws using a handheld glucometer. There were no outliers (ROUT method, Q = 1%) and no severe incidents of hypoglycaemia in these normal, healthy monkeys (Fig. 5c). The lowest detected concentration (73 mg dl^{-1} for subject 3 at 0.5 h) still falls well within the normal fed blood glucose range for cynomolgus macaques[50]. Assuming a similar bioavailability across species and using power laws of allometric scaling, this data suggests that our injectable GLP1–ELP$_{opt}$ depots could provide prolonged release for 3 weeks of glycaemic control in humans. In fact, using equations of allometric scaling, it is possible this construct could even serve as a once-monthly option for diabetic patients, an exciting prospect given that all currently approved formulations require daily or weekly injection[18].

Blood samples from these monkeys were also tested for anti-drug antibodies (ADAs), as immunogenicity is a common hurdle in biologic drug development[51]. Antibodies to a foreign material typically develop in monkeys by day 14 and can begin as early as day 7 post-exposure[51]. To avoid interference from the circulating drug, we compared pre-treatment serum to samples from days 24 and 30. Results show an increase in antibody response over pre-dose levels (Supplementary Fig. 17a–d). Because of this ADA indication, we also performed a pharmacokinetics bioassay. If the ADAs are neutralizing, we would expect to see a discrepancy between levels of GLP1–ELP$_{opt}$ in serum that was quantified by the sandwich ELISA and the levels of functionally active GLP1

assayed in parallel by measuring cAMP generation in GLP1R-expressing cells treated with the serum. The bioassay results were consistent with immunoassay results (Supplementary Fig. 17e,f), indicating that, despite antibody generation, the drug is still active and capable of activating its receptor for nearly three weeks after a single SC injection.
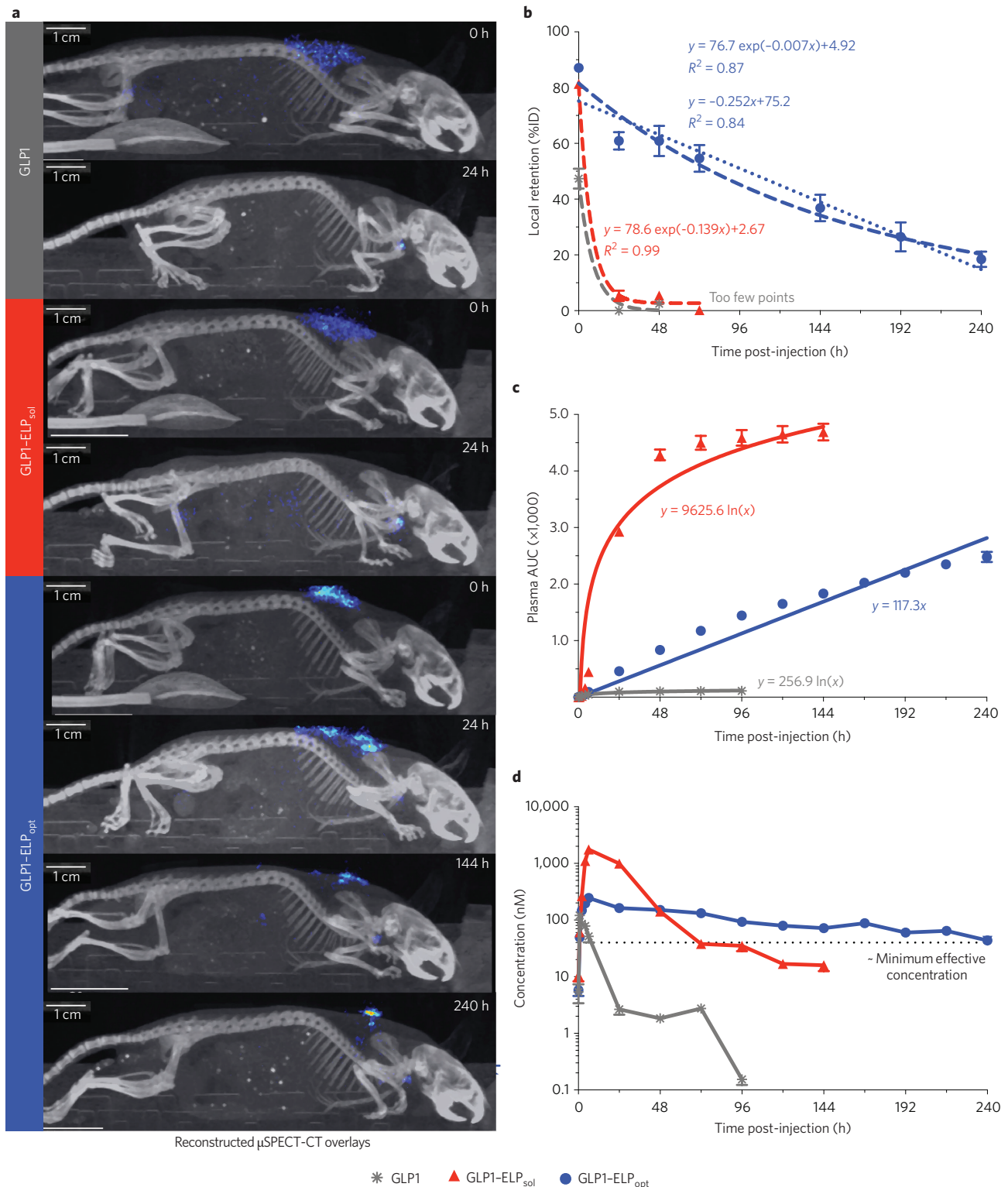

Figure 4 | GLP1–ELP_opt depots persist in the SC space and enhance the drug's pharmacokinetics. a,b, μSPECT-CT images illustrate how long each injected construct remains in the SC space (**a**) and were used to calculate local depot retention at the site of SC injection ($n = 4$) (**b**). **c**, Circulating GLP1–ELP_opt calculated as cumulative AUC versus time can be fit with either linear or logarithmic regression. **d**, Corresponding plasma concentrations after the depot has been absorbed into circulation ($n = 3$) show improved pharmacokinetics with GLP1–ELP_opt. The dashed line represents an approximated minimum effective concentration of GLP1–ELP, calculated with accounting for the reduced activity of the fusions (see Supplementary Section 1.3). Data represent the mean and s.e.m.

Table 3 | Summary of long-term efficacy after eight weeks of treatment with GLP1–ELP_opt.

Treatment group	Number of subjects	HbA1c (%)			Weight (g)		56-day glucose AUC (normalized)
		Day 0	Day 28	Day 56	Day 0	Day 56	
ob/ob mouse model							
GLP1–ELP_opt	5	4.4 ± 0.2	5.0 ± 0.2	5.8 ± 0.2	32.2 ± 1.0	49.3 ± 1.1	0.67 ± 0.01
PBS control	5	4.4 ± 0.1	5.7 ± 0.2	6.5 ± 0.2	31.5 ± 0.7	54.1 ± 0.8	1.00 ± 0.04
DIO mouse model							
GLP1–ELP_opt	5	NM	NM	4.4 ± 0.1	23.1 ± 0.5	25.6 ± 0.9	0.74 ± 0.04
PBS control	5	NM	NM	4.9 ± 0.1	24.0 ± 0.5	32.6 ± 1.4	1.00 ± 0.02

Values reported are the mean and s.e.m.

Discussion

We have shown how GLP1 delivery can be temporally controlled by fusing it to an ELP biopolymer and injecting it as a SC depot that has improved half-life and controlled release features. Our work has identified a framework for the rational and systematic optimization of injectable drug delivery systems at the molecular level—a feature too rarely seen in the design of drug delivery systems. First, we showed that there was an optimal T_t, just below body temperature, which enabled SC depot formation and optimized the extent and duration of release for this application. Second, independent of its impact on the T_t, we found that a $M_w \geq 35$ kDa is needed to prolong circulation and control blood glucose. This is because once a fusion is released from the depot, its M_w controls its time in systemic circulation. For the ELP system investigated here, we found that the diffusive size (R_h) of 20 kDa ELP fusions was too small to retard kidney clearance. Moreover, the T_t values of lower-M_w ELPs had greater dependence on their concentration so that they experienced a greater driving force to dissolve and diffuse into systemic circulation compared to higher-M_w ELPs. This expended GLP1–ELP from the depot more quickly, leading to a reduced duration of glycaemic control.

Importantly, these results demonstrate that systematic molecular optimization of the parameters that control release from an ELP coacervate depot can significantly improve the *in vivo* performance of the fusion. GLP1–ELP_opt provided up to 10 d of glucose control from a single SC injection in three different mouse models of type 2 diabetes (DIO, ob/ob and db/db) and significantly reduced glucose AUC compared to PBS-treated controls. Comparing these results with our own data of this delivery system, the same dose of the first-generation depot-forming GLP1–ELP fusion was only able to achieve 2–3 d of glucose regulation in ob/ob mice[32]. Moreover, our results show superior preclinical efficacy compared to other molecularly engineered GLP1 formulations currently in clinical

use. Specifically, db/db mice treated with Trulicity required twice-weekly treatment[52], whereas we saw 10 d of glucose control in the same model.

Interestingly, the weight loss effects were different across mouse models, with GLP1–ELP_opt treatment effecting weight loss in the DIO model, but weight-neutral or weight gain in the ob/ob and db/db models, respectively. This can be explained by leptin pathway disregulation in the genetic models with homozygous mutation to the leptin protein (ob/ob) or its cognate receptor (db/db). Leptin, the satiety hormone produced by adipocytes, helps to inhibit hunger and regulate energy balance. Our results suggest that an intact leptin pathway is necessary for GLP1 to exert its appetite-suppressing effects in the hypothalamus. This is supported by literature showing that leptin enhances the anorectic and weight loss responses to postprandial incretin signals and, in leptin-receptor-deficient rats, food intake is not suppressed by incretin treatment[53]. With GLP1–ELP_opt treatment, there is a clear trend of decreased weight loss with increasing severity of disease phenotype, from leptin-resistant DIO mice[54] to Lep^ob/ob and LepR^db/db mice.

Fusion to an ELP, whether soluble or depot forming, reduces the activity and bioavailability of GLP1. However, we believe this is an acceptable tradeoff given the improvements made to the peptide's half-life. Pharmacokinetics in mice quantitatively demonstrates that fusion to an ELP increases the $T_{1/2\text{-elim}}$ of GLP1 by over 70-fold, and fusion to a depot-forming ELP provides a mechanism that controls release so that the drug's apparent half-life ($T_{1/2\text{-biol}}$) can be extended far beyond its $T_{1/2\text{-elim}}$. The μ-SPECT-CT imaging confirms that the GLP1–ELP_opt depot was able to sustain release for up to 10 d in mice, with approximately 18% of the injected dose still present in the SC space on day 10. Because of this remaining drug and its long $T_{1/2\text{-biol}}$, this formulation could be a good candidate for dose stacking at the start of treatment to even further prolong the duration of glycaemic control. We also show that the optimized GLP1–ELP depot has
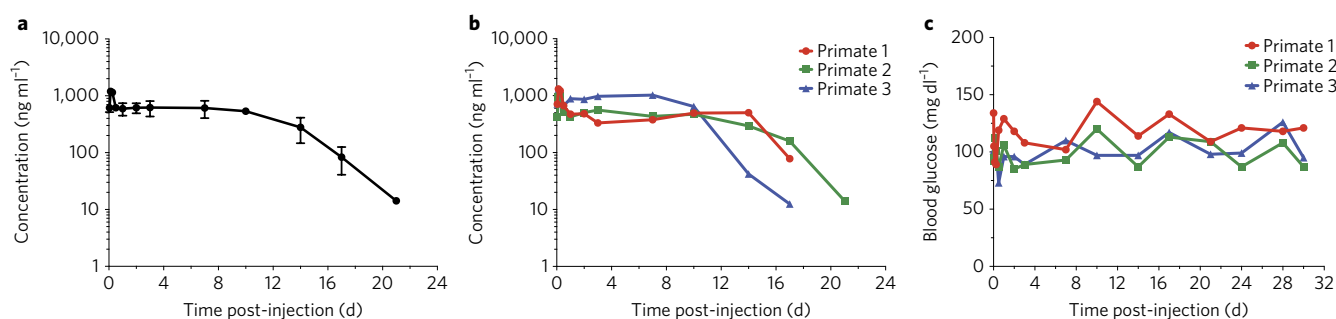
Figure 5 | Injectable SC depots of GLP1–ELP_opt release drug into circulation that can be quantified up to 17–21 days in non-human primates.
a,b, Circulating GLP1–ELP_opt with time following a single SC injection of 10 mg kg⁻¹ shown as mean and s.e.m (**a**) or individual (**b**) concentrations in cynomolgus macaque monkeys (*n* = 3). **c**, Glucose levels remained within a normal range throughout the duration of the experiment for all three subjects, with no incidents of hypoglycaemia.

close to perfect zero-order release kinetics, whereas competing FDA approved formulations, Trulicity and Tanzeum, which rely solely on their fusion partners to extend circulation times, have more rapid and immediate declines in plasma concentration because they do not have a mechanism to sustain release.

Our optimized GLP1–ELP fusion sets itself apart from competing GLP1 molecular delivery technologies by its 10 days of glucose control and zero-order release kinetics in mice. In comparison to preclinical studies of these FDA-approved once-weekly formulations, GLP1–ELP$_{opt}$ has a better pharmacokinetic profile in non-human primates than Trulicity, a once-weekly formulation of GLP1 fused to an Fc domain[55]. In monkeys, plasma levels of Trulicity were only detectable for up to 14 d, remaining constant only for the first 2 d and then dropping steadily with time[55]. With the optimized, depot-forming GLP1–ELP$_{opt}$, we achieved constant levels for the first 14 d (seven times as long as Trulicity) in monkeys and detectable levels of drug for even longer thereafter. When compared with the GLP1–albumin fusion Tanzeum[56], GLP1–ELP$_{opt}$ (10 mg kg^{-1}) was dosed at a five-fold lower level than Tanzeum (50 mg kg^{-1}) in monkeys, according to FDA Access Data.

These comparisons emphasize the power of combining prolonged circulation with a controlled release mechanism in the same delivery platform. Bydureon, which is comprised of the GLP1 analog, exendin-4, formulated in PLGA microspheres[27], is currently the only FDA-approved once-weekly GLP1 receptor agonist that utilizes a controlled-release formulation. While injection of Bydureon, which requires larger needles (smaller gauge) to accommodate the PLGA microspheres[57], can cause patient discomfort, our formulation is soluble at room temperature and is easily injected with standard 29.5 gauge insulin syringes. It also demonstrates minimal lag phase or burst release of drug, features common to PLGA microspheres[58], making it a desirable alternative to Bydureon. Another advantage of GLP1–ELP$_{opt}$ is its ease of recombinant production in *E. coli* with high yield at low cost—unlike Trulicity, which requires more complicated and costly production in mammalian cells (HEK293-EBNA)[55].

While our GLP1–ELP$_{opt}$ formulation holds much clinical promise, a major concern for biologic drugs is the development of antibodies. The drug's long-term efficacy after 2 months of weekly dosing, in addition to its consistent pharmacodynamic profile after repeated injections in mice (Supplementary Fig. 16), indicates an absence of immunoneutralization, and suggests that our construct does not generate a deleterious antibody response. Furthermore, although ADAs were detected in monkeys, they are non-neutralizing and did not prevent the drug from activating its receptor in a pharmacokinetics bioassay. It is also worth noting that, while the monkeys used in this study were naive to our GLP1–ELP fusion, they had been previously used for testing other unknown compounds. Thus, true determination of antibody response warrants testing in fully naive animals, which will be the focus of future studies.

While we focused on optimizing the sustained release capabilities of ELP fusion depots for treating a chronic disease, it is worth noting that this highly tunable approach transcends GLP1 and should be valid for ELP fusions with diverse peptide and protein drugs. Although they require further study of release kinetics and bioavailability, the more hydrophobic and stable ELPs may be suitable for even longer release of biologics that are needed at more modest plasma drug concentrations, such as in inducing immune tolerance, or for applications such as intratumoural drug delivery where local retention of a drug is desirable.

In summary, we have developed a design framework for a biomolecular delivery system that can be systematically optimized at the molecular level. This genetically encoded delivery system controls release, exhibiting zero-order kinetics, and a single injection can maintain circulating levels of GLP1 for 17–21 days in monkeys, which is, to our knowledge, the longest duration reported for a recombinant injectable delivery system. On the basis of allometric scaling using a power function with body weight[49,59], mouse and monkey pharmacokinetic data suggest that this delivery system may be suitable for once-monthly dosing in humans. We estimate that GLP1–ELP$_{opt}$ would have a terminal half-life in humans greater than 100 h and a clearance of approximately 17 ml h^{-1}. Preclinical data presents compelling evidence that this construct would require no more than two injections a month for humans, and possibly as few as one per month, especially given the dose-stacking potential of this system. Such an improvement could vastly improve patient quality of life by reducing the frequency and pain of injections while also providing clinicians with the means to further decouple patient compliance from therapeutic outcome.

Methods

Synthesis of GLP1–ELP fusions. For each construct, oligomers were purchased from Integrated DNA Technologies as starting material and recombinantly engineered into separate pET24 plasmids (EMD Millipore). The ELP and GLP1 peptide genes were fused using plasmid reconstruction by recursive directional ligation (PRe-RDL)—an iterative gene assembly method that employs type IIs restriction endonucleases to seamlessly assemble the synthetic genes that encode repetitive polypeptides such as ELPs[60].

The GLP1 used in all studies reported here has been sequence-engineered to incorporate mutations at the genetic level to improve its stability. An Ala to Gly mutation at position 8 makes GLP1 DPP-IV resistant[61] because the enzyme only recognizes and cleaves N-terminal dipeptides where the second residue is either Ala or Pro[62]. Wild-type GLP1 is comprised of amino acids 7–37; by convention, the initial N-terminal His residue is numbered 7 as a result of its initial discovery as a longer proglucagon fragment whose initial 6 residues are cleaved during further processing in the gut[63]. We also added two extra residues at the N-terminus, an Ala-Ala leader, which is cleaved by endogenous DPP-IV in circulation. This DPP-IV cleavage serves to activate, rather than inactive, the drug by releasing the dipeptide and freeing the N-terminus for receptor activation. A Gly to Glu mutation at position 22 stabilizes the alpha-helical structure of GLP1[64] and an Arg to Ala mutation at position 36 prevents premature cleavage of the peptide from its ELP carrier in the SC space by ubiquitous arginine targeting proteases[65]. The full-length sequence can be found in the Supplementary Information.

Expression and purification of GLP1–ELPs. The gene for each GLP1–ELP fusion, inserted under control of a T7 promoter in a pET24 plasmid, was transformed into Ultra BL21 (DE3) competent *E. coli* cells (Edge BioSystems). The cells were grown at 37 °C in TB Dry (MO Bio) and expressed by induction of the T7 RNA polymerase with 0.5 mM isopropyl β-D-1-thiogalactopyranoside (IPTG). Cells were lysed using sonication pulsed at 10 s on and 40 s off, for a total sonication time of 3 min. DNA was removed by adding 1 ml of 20 w/v% polyethylenimine (PEI) per litre culture and centrifuging at 24,000g for 10 min. Fusions were subsequently purified through inverse transition cycling (ITC) by exploiting the phase transition behaviour of the ELP[66]. Purity was confirmed by SDS–PAGE on 4–20% Tris gradient gels (Bio-Rad) negatively stained with 0.5 M CuCl$_2$. Protein bands were compared to a standard ladder (Precision Plus Protein Kaleidoscope, Bio-Rad) to verify size.

Phase behaviour characterization. The LCST phase behaviour of each fusion was characterized using a temperature-controlled UV-vis spectrophotometer (Cary 300 Bio, Varian Instruments) to measure the change in optical density at 350 nm as the sample was heated at a rate of 1 °C min^{-1}. A sharp increase in absorbance indicates a phase transition of ELP from a soluble state to micron-sized aggregates. The T_t was defined as the inflection point of the turbidity versus temperature curve, and calculated as the maximum of the first derivative. The 350 nm absorbance was also measured as temperature was ramped back down at 1 °C min^{-1} to confirm reversibility of the phase behaviour, an attribute critical for facilitating release of drug from the depot into circulation.

Light scattering. Dynamic light scattering (DLS) was performed on a temperature-controlled DynaPro Microsampler (Wyatt Technologies) to quantify the hydrodynamic radius (R_h) of each GLP1–ELP fusion. Constructs were measured at 1 mg ml^{-1} in PBS at 15 °C after filtering through a 0.22 µm PVDF filter (Durapore). For three technical replicates, 18 repeat measurements of 5 s acquisitions were analysed by applying a regularization fit to the scattering intensity autocorrelation function for Rayleigh spheres.

***In vitro* activity assay.** The *in vitro* activity of GLP1–ELP fusions were quantified by measuring the increase in cyclic adenosine monophosphate (cAMP) levels in baby hamster kidney (BHK) cells that were stably transfected to constitutively express rat GLP1 receptor (GLP1R) on the cell surface[35]. The transfected cells were a generous gift from Daniel Drucker (University of Toronto). GLP1R is a

G-protein-coupled receptor whose downstream signalling is mediated by a second messenger cAMP cascade, resulting in insulin secretion. Thus, the cAMP level is often used as a measure of receptor activation. Prior to performing the assay, GLP1–ELP fusions at 50 μM concentration were incubated overnight with 0.01 μg human DPP-IV (Prospec Bio) to cleave the protective Ala-Ala leader and expose an active N-terminus. Cells were passaged at least once prior to performing the assay and were cultured in high glucose DMEM (Thermo Fisher, 11960-044) supplemented with 10% fetal bovine serum, 100 U ml^{-1} penicillin, 100 μg ml^{-1} streptomycin and 50 μg ml^{-1} G418 (Thermo Fisher). Cells were seeded without G418 on 24-well plates at 30,000 cells per well in 0.5 ml media and incubated at 37 °C for 24–48 h, until reaching approximately 80% confluence. To prevent cAMP degradation, 250 μM 3-isobutyl-1-methylxanthine (IBMX) was added to each well and incubated for 1 h prior to beginning the assay. Cells were then treated for 15 min with 10 μl of GLP1–ELP fusion or native GLP1 control over a log-range of concentrations. For each construct, three tubes were individually prepared at the maximum concentration and then serial dilutions were made for each. Intracellular cAMP level for each treatment and concentration was assayed in triplicate using a colorimetric, competitive binding, enzyme-linked immunosorbent assay (ELISA) carried out with the high-sensitivity acetylated cAMP protocol, according to kit instructions (Enzo Life Sciences). The 650 nm absorbance in each well was subtracted from its 405 nm absorbance. After subtracting the mean cAMP level of PBS-treated control wells, the dose-response data was fit using a four-parameter logistic, nonlinear regression model (GraphPad Prism 6). The calculated EC$_{50}$ values represent the half-maximal effective concentration.

***In vivo* studies in mice.** All experimental procedures were conducted under protocols approved by the Duke Institutional Animal Care and Use Committee (IACUC). Constructs were endotoxin purified prior to injection by passing the solution through a sterile 0.22 μm Acrodisc filter comprised of a positively charged and hydrophilic Mustang E membrane (Pall Corporation). Mice were group housed in a room with a controlled photoperiod (12 h light/12 h dark cycle) and allowed at least 1 week to acclimate to the facilities prior to that start of procedures. Animals had *ad libitum* access to water and food. Mice were fed a standard rodent diet (LabDiet 5001) unless otherwise indicated and observed daily.

Pharmacodynamics. For evaluating the ELP series with variable T_t or M_w, 6-week-old C57Bl/6J male mice (stock number 000664, Jackson Laboratories) were purchased. Mice ($n = 5$ to 6 per treatment group) were immediately placed on a 60 kcal% fat diet (Research Diets D12492) and allowed 1 week to acclimate to facilities. Treatment groups were randomized. On day 0, initial body weight and blood glucose were measured; then mice were SC injected with GLP1–ELP fusions (700 nmol kg^{-1}, 200–500 μM) or an equivalent volume of PBS kept on ice. A small nick of the tail vein was made with a lancet. The first drop of blood was wiped clean and the second drop was measured using an AlphaTrak2 handheld glucometer (Abbott), which measures blood glucose using the glucose oxidase method. Glucose measurements were taken periodically throughout day 0 and then every 24 h post-injection.

For efficacy and dose response studies in diet-induced obese (DIO) subjects, 6-week-old male C57Bl/6J mice ($n = 5$) were maintained on the high-fat diet for 11 weeks prior to treatment. For the dose response study, GLP1–ELP concentration was kept constant and injection volume was adjusted for the various treatment groups. For efficacy studies in strains with more progressed diabetes, male mice homozygous for the spontaneous Lep^{ob} mutation (ob/ob, strain 000632) or the Lepr^{db} mutation (db/db, strain 000697) were used. These mice were treated with the same dose and measured as previously described.

Long-term efficacy. Six-week-old male C57BL/6J mice ($n = 5$, stock number 000664) placed on a 60 kcal% fat diet were injected with GLP1–ELP every 6 days for 8 weeks (700 nmol kg^{-1}, 200 μM). A1C was measured at the end of the study using a handheld A1cNow meter (Bayer), which uses a photometric immunoassay platform. Four-week-old ob/ob mice ($n = 4$, stock number 000632) were purchased from Jackson Laboratories and injected with GLP1–ELP every 7 days (700 nmol kg^{-1}, 200 μM). Blood glucose and weight were measured periodically and glycosylated haemoglobin (%HbA1c) was measured using a monoclonal antibody agglutination reaction automated by a DCA Vantage Analyzer (Siemens).

Intraperitoneal glucose tolerance test (IPGTT). During the first week of the long-term study in ob/ob mice ($n = 4$), two IPGTTs were performed. Mice received a single SC injection of GLP1–ELP$_{opt}$ or equivalent volume of PBS on day 0. At 66 h post-injection, mice were fasted for 6 h and then challenged with an intraperitoneal (IP) injection of 1 g kg^{-1} 10 w/v% sterile glucose (Sigma-Aldrich). At 72 h post-injection, blood glucose was measured at 0, 10, 20, 40, 60, 90, 120 and 170 min after glucose administration. This procedure was repeated at 144 h post-injection for a day 6 IPGTT. The glucose meter is unable to read glucose levels below 20 or above 750 mg dl^{-1}. For measurements where the meter read 'HI', maximal values of 750 mg dl^{-1} were substituted to enable statistical analysis.

Imaging with μSPECT-CT. GLP1–ELP$_{opt}$ and a soluble control, GLP1–ELP$_{sol}$, with the same number of VPGXG repeats (310 μM), as well as custom-ordered

modified GLP1 peptide (75 μM, Anaspec), were radiolabelled with Na^{125}I (Perkin Elmer) using the Chizzonite indirect method[67] for protein iodination to minimize oxidative damage to the peptide[68]. Briefly, in IODOGEN tubes (Thermo Fisher) pre-wetted with 50 μl of PBS, Na^{125}I was added to each construct at a molar ratio of 1:250 iodine to GLP1. After 5–10 min on ice, the oxidation reaction was quenched with the addition of 10 μl 0.1% trifluoroacetic acid (TFA). Free Na^{125}I was removed using overnight dialysis in 500 ml sterile PBS (Sigma). The final activities were 1.18 μCi μl^{-1} free peptide (37.5 μM), 0.49 μCi μl^{-1} GLP1–ELP$_{sol}$ (200 μM) and 0.72 μCi μl^{-1} GLP1–ELP$_{opt}$ (200 μM). An identical procedure was performed using non-radioactive NaI, after which concentrations were determined by measuring 280 nm absorbance on a NanoDrop 1000 and successful iodination was confirmed with matrix-assisted laser desorption and ionization mass spectrometry (MALDI–MS) on trypsin digested samples (Supplementary Fig. 1). For the tryptic digest, samples were diluted to 25 μM in 50 mM ammonium bicarbonate and incubated with 0.2 μg MS grade trypsin (ThermoFisher Scientific) for 4 h at 37 °C. Samples were diluted 1:10 in 10 mg ml^{-1} 4-hydroxycinnamic acid (HCCA) matrix prior to analysis with a DE-Pro MALDI-MS (Applied Biosystems).

Six-week-old male ob/ob mice ($n = 4$) were treated with a single SC injection of radiolabelled GLP1 (30 nmol kg^{-1}), GLP1–ELP$_{sol}$ (700 nmol kg^{-1}), or GLP1–ELP$_{opt}$ (700 nmol kg^{-1}) and imaged with a U-SPECT-II/CT imaging system using a 0.350 collimator (MILabs B.V., Utrecht, Netherlands) courtesy of G. Al Johnson at Duke University's Center for *In Vivo* Microscopy (CIVM). Anaesthesia was maintained with a 1.6% isoflurane feed at an O$_2$ flow rate of 0.6 l min^{-1}. All 20 min SPECT images were reconstructed at 0.2 mm voxel size with MILabs proprietary software without decay correction and centered on the ^{125}I photon range (15–45 keV). These reconstructed SPECT images were then registered with their corresponding CT scans (615 μA, 65 kV) to provide spatial alignment for anatomical reference. For each subject, at each time point, the total photon intensity was calculated using ImageJ for (1) the entire image and (2) for an ROI selected to contain the depot and ensure exclusion of the thyroid, bladder and pancreas. Depot retention was calculated by normalizing the depot ROI intensity to that subject's 0 h full image intensity.

Pharmacokinetics and biodistribution in mice. The same mice from the μSPECT-CT study treated with radiolabelled constructs were also used to study depot pharmacokinetics in parallel. Following SC treatment, total body activity was measured using an AtomLab 400 dose calibrator (Biodex) and 10 μl of blood was collected from a tail vein nick into 90 μl of 1,000 U ml^{-1} heparin. Total body activity measurements and blood draws were repeated at 0.75, 2, 4 and 6 h post-injection and every 24 h thereafter up to 144 h in the GLP1 and GLP1–ELP$_{sol}$ groups and to 240 h in the GLP1–ELP$_{dep}$ group. Upon completion of the study, mice in the GLP1–ELP$_{dep}$ group were euthanized and dissected. Local SC injection site skin and fat were excised in addition to distal skin, distal fat, flank muscle, heart, lungs, thyroid, liver, pancreas, spleen, stomach and kidneys. A separate cohort of mice was used to measure the pharmacokinetics of the same constructs following a 10 nmol kg^{-1} IV bolus injection of radiolabelled drug diluted to 1 μM to prevent phase transition. 10 μl of blood was collected into 1000 U ml^{-1} heparin solution at 40 s, 10 min, 45 min, 1.5 h, 3 h, 6 h, 12 h, 18 h, 24 h, 36 h, 48 h and 54 h post-injection.

Radioactivity of the dissected organs and all blood samples was quantified with a Wallac 1282 Gamma Counter (Perkin Elmer). To calculate the half-life, raw CPM values of blood samples were plotted against time and fit to a one-phase exponential decay function in GraphPad Prism 6 using data points in the elimination phase of the pharmacokinetic curve for the IV study and after t_{max} for the SC study. These curves were fit for each subject individually because of slightly variable time points. The parameters presented are the average values within each treatment group and the standard error of the mean (SEM).

For quantification of circulating drug concentrations, the gamma count for each sample was converted to nanomolar concentration using a set of standards and then dividing by the blood sample volume (10 μl). For the IV data, $T_{1/2\text{-elim}}$ was calculated as $\ln(2)/k_e$, where k_e was found by fitting a line of exponential decay to the elimination phase of the pharmacokinetic curve generated from raw CPM values (45 min to 48 h range for the fusions and 2 min to 1.5 h range for the peptide). For the SC pharmacokinetic data, the same fit was used covering time points after C_{max} had been reached to calculate the biological half-life ($T_{1/2\text{-biol}}$), which accounts for the controlled release and slowed absorption from the SC route of administration. In order to quantify C_{max} and compare the drug AUC for all three constructs, the detected counts CPM were converted to molar concentration using a standard curve built from aliquots of each injected construct, whose activities and concentrations were known. Bioavailability (F) was calculated as the ratio of dose-normalized AUC$_{SC}$ to AUC$_{IV}$, using the equation: F = (AUC$_{SC}$ × dose$_{IV}$)/(AUC$_{IV}$ × dose$_{SC}$). Clearance (CL) was calculated as (dose × F)/AUC where F = 1 for a bolus IV injection. Although there have been few reports of a minimum effective concentration of GLP1 in mice, we approximated a value (33 nM) based on a study of how the insulin-stimulating effects of GLP1 are dependent on IV dose[69] in conjunction with a study that involved measuring plasma GLP1 levels after IV administration[70]. The calculation of this value is discussed in more detail in the Supplementary Information. The 40 nM value also correlates with the concentration at which a maximum GLP1 receptor response is observed for fusion treatment *in vitro*.

Histology of the injection site. Five-week-old male ob/ob mice were allowed one week to acclimate to the facilities. On the day of injection, mice were anaesthetized with isoflurane and shaved across their backs. Two circles, approximately 12 mm in diameter, were marked bilaterally with permanent marker and injected in the center of the circle at 50 mg kg^{-1} or an equal volume of saline. Injections of PBS, GLP1–ELP$_{opt}$ or PLGA microspheres 50 μm in diameter (Sigma) were randomized, but stratified to ensure that no mouse received the same injection type bilaterally. After 5 days, the mice were euthanized and the skin was dissected. A 12 mm biopsy punch (Electron Microscopy Sciences) was used to remove the area indicated by the permanent marker. The skin was cut in half and placed in 10% neutral buffered formalin. After paraffin embedding, three 5 μm sections were taken from the midline cut, spaced apart by 50 μm. These sections were stained with H&E and imaged using a Zeiss laser microdissection and capture microscope equipped with an AxioCam ICc3 color camera. The slides were inspected and analysed by a certified pathologist who was blinded to the groups.

In vivo pharmacokinetics study in monkeys. For detailed information on production and purification of GLP1–ELP$_{opt}$ for primate testing, see Supplementary Information. Briefly, purity was assessed by SDS–PAGE, size-exclusion high-performance liquid chromatography (SEC–HPLC) (SI Fig. 2) and reversed-phase (RP) HPLC (Supplementary Fig. 3). The peptide fusion was verified with electrospray ionization mass spectrometry (ESI–MS) (Supplementary Fig. 4) and N-terminal sequencing (Supplementary Table 1). Activity was assessed using a GLP1-receptor-expressing Chinese hamster ovary (CHO) cell line with a cAMP fluorescent assay kit (Supplementary Fig. 5).

To evaluate the pharmacokinetic profile of the fusion in primates, GLP1–ELP$_{opt}$ was sent to the In-Life Testing Facility at the Sinclair Research Center for testing. Animals were group housed and only temporarily caged in single housing for feeding, study procedures and clinical observation. The housing room was maintained between 18 °C and 29 °C on a controlled photoperiod (12 h light/12 h dark cycle). Animals had *ad libitum* access to water and were fed a maintenance diet of Teklad High Fiber Diet with supplemental fresh fruits and vegetables. Animals were observed twice daily and physically examined during the period of acclimation. Food consumption was qualitatively monitored daily and weight was measured during acclimation, prior to dose administration, and then weekly thereafter. Following completion of the study, animals were released to the Sinclair Research Center open colony.

After a 5-day acclimation period, 3 male protein-naive cynomologus macaques were given a single SC injection of GLP1–ELP$_{opt}$ at a dose of 10 mg kg^{-1} (150 nmol kg^{-1}), at a concentration of 400 μM. These monkeys ranged from 43 to 73 months of age and weighed between 3.33 and 4.42 kg. Following administration of this single dose, serial blood collections were taken at 1, 3, 6, 12, 24, 48, 72, 168, 240, 336, 408, 504, 576, 672 and 720 h post-injection via direct venipuncture into sterile vacutainers without coagulant. The samples were centrifuged at 1,300g for 15 min at 4 °C and serum was stored at −70 °C in a cryovial. These samples were analysed by ELISA at PhaseBio Pharmaceuticals using a biotinylated anti-GLP1 capture antibody (Antibody Shop HYB147-12B) mixed at a 60:40 ratio with biotinylated BSA and an anti-ELP detection antibody labelled with Alexa 647 (in-house IgY generated in chicken, diluted to 20 nM in Rexxip F). Standards, samples and reagents were loaded onto the Gyrolab immunoassay system utilizing a three-step method. The limit of quantification for this test was 2.44 ng ml^{-1} GLP1–ELP.

Anti-drug antibodies were measured semi-quantitatively using two separate assays—one for antibodies developed against GLP1–ELP$_{opt}$ and a second for those reactive against native GLP1—performed both with and without competition with soluble drug or peptide. For the anti-drug assay, GLP1–ELP$_{opt}$ was bound at 1 μg per well in a 96-well black microtitre plate. The plate was washed and blocked in a casein-based blocking buffer. Serum samples from pre-dosing as well as days 24 and 30 were diluted 1:50 in either the same buffer or buffer containing the drug, and incubated with shaking. After incubation, all samples were applied to the plate and incubated again at room temperature with shaking. Plates were washed with Tris-buffered saline with Tween20 (TBST) and then protein A/G conjugated to HRP was added and left for ~60 min. After a final wash step, QuantaBlu (Thermo Fisher Scientific) fluorescent substrate was added. Plates were read on a Molecular Devices Spectramax M5 microplate reader. Surrogate controls for this assay included sheep polyclonal anti-ELP antibody (PhaseBio). The second assay for GLP1 specificity involved binding 50 ng per well biotinylated GLP1 to a 96-well streptavidin black microtitre plate and then performing a wash and blocking step with SuperBlock blocking buffer (Thermo Fisher Scientific). The same serum samples, diluted 1:50 in buffer alone or buffer with GLP1, were incubated with shaking and then applied to the plate and incubated for another 60–65 min. The plates were washed, bound with QuantaBlue, and detected in the same manner as for the first assay. The surrogate control for this assay was a mouse monoclonal anti-GLP1 antibody. Both these assay formats were repeated using HRP-labelled monkey anti-IgM, IgG and IgA as the detection reagent. Unfortunately, attempts to isotype the sample response was unsuccessful due to high levels of cross-reactivity in isotype-specific antibodies. This experiment may have been confounded because non-naive monkeys were used for this study and the previously tested compounds in the monkeys are unknown.

A parallel pharmacokinetics bioassay was conducted using GLP1R-expressing CHO cells and a cAMP assay. Cells were plated on 96-well tissue culture treated plates and incubated for 24 h at 37 °C. GLP1–ELP$_{opt}$ was diluted to 1,000 nM in 100 μl of water and incubated with 1 μg DPPIV overnight in order to cleave the Ala-Ala leader and allow for receptor binding. A standard curve for cAMP generation was made using this activated drug diluted in pre-dose serum from each primate. As per the kit's recommended protocol, cell media was aspirated from the plates and 40 μl assay buffer was added to each well followed by 5 μl of each standard or serum sample from individual days of the pharmacokinetic study and for each primate subject. The plates were incubated at 37 °C for 30min. Following the incubation, 15 μl cAMP antibody reagent and 60 μl cAMP working detection solution were added to each well. Plates were incubated at room temperature for 1hr protected from light. Then, 60 μl of cAMP solution A was added to each well and the plates were incubated for 3 h at room temperature protected from light. After this final incubation, the plates were read on a luminescence plate reader at 1 s per well. Using a four-parameter curve fit, the drug (diluted in monkey 1M1, 1M2 or 1M3 predose serum) were plotted as signal versus concentration. Quantification of active drug in serum samples was determined from sample dilutions falling within the linear range generated from the calibration curve.

Statistical analysis. Experimental numbers for both *in vitro* and *in vivo* studies were selected based on knowledge gleaned from previous experiments or other published data. Because of the small sample size ($n \leq 6$), normality of groups was not tested. Variance across groups was similar except in untreated versus treated *in vivo* groups, which is not unexpected given the lack of glucose control in the mouse models tested. All data are presented as mean and SEM unless otherwise noted. Blood glucose and per cent change in weight studies were analysed using repeated measures ANOVA, followed by lower-order ANOVA and Dunnett's Test for multiple comparisons. Glucose AUC values were calculated using the trapezoidal method and then compared using a one-way ANOVA followed by either Tukey's or Bonferroni's multiple comparisons, as indicated. For comparing two groups, two-tailed Student's *t*-tests were used. For animal experiments, groups were randomized using a list generator on www.random.org. No blinding was performed. All analyses and data processing were performed using GraphPad Prism 6 software.

Data availability. The authors declare that all data supporting the findings of this study are available within the paper and its Supplementary Information. Source data for the figures in this study are available in figshare with the identifier doi:10.6084/m9.figshare.4903931 (ref.[71]).

References

1. *National Diabetes Statistics Report: Estimates of Diabetes and Its Burden in the United States, 2014* (Centers for Disease Control and Prevention, 2014).
2. Bailey, C. J. The current drug treatment landscape for diabetes and perspectives for the future. *Clin. Pharmacol. Therap.* **98,** 170–184 (2015).
3. Inzucchi, S. E. *et al.* Management of hyperglycaemia in type 2 diabetes, 2015: a patient-centred approach. Update to a position statement of the American Diabetes Association and the European Association for the Study of Diabetes. *Diabetologia* **58,** 429–442 (2015).
4. Bell, G. I., Santerre, R. F. & Mullenbach, G. T. Hamster preproglucagon contains the sequence of glucagon and two related peptides. *Nature* **302,** 716–718 (1983).
5. Mojsov, S. *et al.* Preproglucagon gene expression in pancreas and intestine diversifies at the level of post-translational processing. *J. Biol. Chem.* **261,** 11880–11889 (1986).
6. Mortensen, K., Christensen, L. L., Holst, J. J. & Orskov, C. GLP-1 and GIP are colocalized in a subset of endocrine cells in the small intestine. *Reg. Pept.* **114,** 189–196 (2003).
7. Flint, A., Raben, A., Astrup, A. & Holst, J. J. Glucagon-like peptide 1 promotes satiety and suppresses energy intake in humans. *J. Clin. Invest.* **101,** 515–520 (1998).
8. Meeran, K. *et al.* Repeated intracerebroventricular administration of glucagon-like peptide-1-(7-36) amide or exendin-(9-39) alters body weight in the rat. *Endocrinology* **140,** 244–250 (1999).
9. Drucker, D. J. Glucagon-like peptide-1 and the islet beta-cell: augmentation of cell proliferation and inhibition of apoptosis. *Endocrinology* **144,** 5145–5148 (2003).
10. Qualmann, C., Nauck, M. A., Holst, J. J., Orskov, C. & Creutzfeldt, W. Insulinotropic actions of intravenous glucagon-like peptide-1 (GLP-1) [7-36 amide] in the fasting state in healthy subjects. *Acta Diabet.* **32,** 13–16 (1995).
11. Meloni, A. R., DeYoung, M. B., Lowe, C. & Parkes, D. G. GLP-1 receptor activated insulin secretion from pancreatic beta-cells: mechanism and glucose dependence. *Diabet. Obes. Metab.* **15,** 15–27 (2013).

12. Rachman, J. *et al.* Normalization of insulin responses to glucose by overnight infusion of glucagon-like peptide 1 (7-36) amide in patients with NIDDM. *Diabetes* **45**, 1524–1530 (1996).

13. Rachman, J., Barrow, B. A., Levy, J. C. & Turner, R. C. Near-normalisation of diurnal glucose concentrations by continuous administration of glucagon-like peptide-1 (GLP-1) in subjects with NIDDM. *Diabetologia* **40**, 205–211 (1997).

14. Quddusi, S., Vahl, T. P., Hanson, K., Prigeon, R. L. & D'Alessio, D. A. Differential effects of acute and extended infusions of glucagon-like peptide-1 on first- and second-phase insulin secretion in diabetic and nondiabetic humans. *Diabet. Care* **26**, 791–798 (2003).

15. Nauck, M. A. *et al.* Normalization of fasting hyperglycaemia by exogenous glucagon-like peptide 1 (7-36 amide) in type 2 (non-insulin-dependent) diabetic patients. *Diabetologia* **36**, 741–744 (1993).

16. Vilsboll, T., Agerso, H., Krarup, T. & Holst, J. J. Similar elimination rates of glucagon-like peptide-1 in obese type 2 diabetic patients and healthy subjects. *J. Clin. Endocrinol. Metab.* **88**, 220–224 (2003).

17. Deacon, C. F., Johnsen, A. H. & Holst, J. J. Degradation of glucagon-like peptide-1 by human plasma *in vitro* yields an N-terminally truncated peptide that is a major endogenous metabolite *in vivo*. *J. Clin. Endocrinol. Metab.* **80**, 952–957 (1995).

18. Gilroy, C. A., Luginbuhl, K. M. & Chilkoti, A. Controlled release of biologics for the treatment of type 2 diabetes. *J. Con. Rel.* **240**, 151–164 (2015).

19. Drucker, D. J. & Nauck, M. A. The incretin system: glucagon-like peptide-1 receptor agonists and dipeptidyl peptidase-4 inhibitors in type 2 diabetes. *Lancet* **368**, 1696–1705 (2006).

20. Jimenez-Solem, E., Rasmussen, M. H., Christensen, M. & Knop, F. K. Dulaglutide, a long-acting GLP-1 analog fused with an Fc antibody fragment for the potential treatment of type 2 diabetes. *Curr. Opin. Mol. Therap.* **12**, 790–797 (2010).

21. Matthews, J. E. *et al.* Pharmacodynamics, pharmacokinetics, safety, and tolerability of albiglutide, a long-acting glucagon-like peptide-1 mimetic, in patients with type 2 diabetes. *J. Clin. Endocrinol. Metab.* **93**, 4810–4817 (2008).

22. Yu, L. *et al. In vitro* and *in vivo* evaluation of a once-weekly formulation of an antidiabetic peptide drug Exenatide in an injectable thermogel. *J. Pharm. Sci.* **102**, 4140–4149 (2013).

23. Chen, Y. P. *et al.* Injectable and thermosensitive hydrogel containing Liraglutide as a long-acting antidiabetic system. *ACS Appl. Mater. Inter.* **8**, 30703–30713 (2016).

24. Gedulin, B. R. *et al.* Dose-response for glycaemic and metabolic changes 28 days after single injection of long-acting release exenatide in diabetic fatty Zucker rats. *Diabetologia* **48**, 1380–1385 (2005).

25. Kim, D. *et al.* Effects of once-weekly dosing of a long-acting release formulation of exenatide on glucose control and body weight in subjects with type 2 diabetes. *Diab. Care* **30**, 1487–1493 (2007).

26. Schwendeman, S. P., Shah, R. B., Bailey, B. A. & Schwendeman, A. S. Injectable controlled release depots for large molecules. *J. Con. Rel.* **190**, 240–253 (2014).

27. DeYoung, M. B., MacConell, L., Sarin, V., Trautmann, M. & Herbert, P. Encapsulation of exenatide in poly-(D,L-lactide-*co*-glycolide) microspheres produced an investigational long-acting once-weekly formulation for type 2 diabetes. *Diab. Technol. Ther.* **13**, 1145–1154 (2011).

28. MacEwan, S. R. & Chilkoti, A. Elastin-like polypeptides: biomedical applications of tunable biopolymers. *Biopolymers* **94**, 60–77 (2010).

29. Chilkoti, A., Christensen, T. & MacKay, J. A. Stimulus responsive elastin biopolymers: applications in medicine and biotechnology. *Curr. Opin. Chem. Biol.* **10**, 652–657 (2006).

30. Cho, Y. H. *et al.* Effects of Hofmeister anions on the phase transition temperature of elastin-like polypeptides. *J. Phys. Chem. B* **112**, 13765–13771 (2008).

31. Amiram, M., Luginbuhl, K. M., Li, X., Feinglos, M. N. & Chilkoti, A. A depot-forming glucagon-like peptide-1 fusion protein reduces blood glucose for five days with a single injection. *J. Con. Rel.* **172**, 144–151 (2013).

32. Amiram, M. *Glucagon-Like Peptide-1 Depots for the Treatment of Type-2 Diabetes.* PhD thesis, Duke Univ. (2012).

33. Trammell, R. A., Cox, L. & Toth, L. A. Markers for heightened monitoring, imminent death, and euthanasia in aged inbred mice. *Compar. Med.* **62**, 172–178 (2012).

34. Runge, S. *et al.* Differential structural properties of GLP-1 and exendin-4 determine their relative affinity for the GLP-1 receptor N-terminal extracellular domain. *Biochemistry* **46**, 5830–5840 (2007).

35. Baggio, L. L., Huang, Q., Brown, T. J. & Drucker, D. J. A recombinant human glucagon-like peptide (GLP)-1-albumin protein (albugon) mimics peptidergic activation of GLP-1 receptor-dependent pathways coupled with satiety, gastrointestinal motility, and glucose homeostasis. *Diabetes* **53**, 2492–2500 (2004).

36. Madsbad, S. *et al.* An overview of once-weekly glucagon-like peptide-1 receptor agonists-available efficacy and safety data and perspectives for the future. *Diab. Obes. Metab* **13**, 394–407 (2011).

37. Chae, S. Y. *et al.* Pharmacokinetic and pharmacodynamic evaluation of site-specific PEGylated glucagon-like peptide-1 analogs as flexible postprandial-glucose controllers. *J. Pharm. Sci.* **98**, 1556–1567 (2009).

38. McDaniel, J. R., Radford, D. C. & Chilkoti, A. A unified model for *de novo* design of elastin-like polypeptides with tunable inverse transition temperatures. *Biomacromolecules* **14**, 2866–2872 (2013).

39. Brenner, B. M., Hostetter, T. H. & Humes, H. D. Glomerular permselectivity: barrier function based on discrimination of molecular size and charge. *Am. J. Physiol.* **234**, 455–460 (1978).

40. Waldmann, T. A., Strober, W. & Mogielnicki, R. P. The renal handling of low molecular weight proteins. II. Disorders of serum protein catabolism in patients with tubular proteinuria, the nephrotic syndrome, or uremia. *J. Clin. Invest.* **51**, 2162–2174 (1972).

41. Pisal, D. S., Kosloski, M. P. & Balu-Iyer, S. V. Delivery of therapeutic proteins. *J. Pharm. Sci.* **99**, 2557–2575 (2010).

42. Caliceti, P. & Veronese, F. M. Pharmacokinetic and biodistribution properties of poly(ethylene glycol)-protein conjugates. *Adv. Drug Deliv. Rev.* **55**, 1261–1277 (2003).

43. Yamaoka, T., Tabata, Y. & Ikada, Y. Distribution and tissue uptake of poly(ethylene glycol) with different molecular weights after intravenous administration to mice. *J. Pharm. Sci.* **83**, 601–606 (1994).

44. Armstrong, J. K., Wenby, R. B., Meiselman, H. J. & Fisher, T. C. The hydrodynamic radii of macromolecules and their effect on red blood cell aggregation. *Biophys. J.* **87**, 4259–4270 (2004).

45. Purtell, J. N., Pesce, A. J., Clyne, D. H., Miller, W. C. & Pollak, V. E. Isoelectric point of albumin: effect on renal handling of albumin. *Kidney Int.* **16**, 366–376 (1979).

46. Dubuc, P. U., Scott, B. K. & Peterson, C. M. Sex-differences in glycated hemoglobin in diabetic and nondiabetic C57bl/6 mice. *Diab. Res. Clin. Pr.* **21**, 95–101 (1993).

47. Vanputten, L. M. The life span of red cells in the rat and the mouse as determined by labeling with Dfp32 *in vivo*. *Blood* **13**, 789–794 (1958).

48. Shemin, D. & Rittenberg, D. The life span of the human red blood cell. *J. Biol. Chem.* **166**, 627–636 (1946).

49. Mahmood, I. Application of allometric principles for the prediction of pharmacokinetics in human and veterinary drug development. *Adv. Drug Deliv. Rev.* **59**, 1177–1192 (2007).

50. Lapin, B. A., Gvozdik, T. E. & Klots, I. N. Blood glucose levels in rhesus monkeys (*Macaca mulatta*) and cynomolgus macaques (*Macaca fascicularis*) under moderate stress and after recovery. *Bull. Exp. Biol. Med.* **154**, 497–500 (2013).

51. Ponce, R. *et al.* Immunogenicity of biologically-derived therapeutics: assessment and interpretation of nonclinical safety studies. *Regul. Toxicol. Pharm.* **54**, 164–182 (2009).

52. Glaesner, W. *et al.* Engineering and characterization of the long-acting glucagon-like peptide-1 analogue LY2189265, an Fc fusion protein. *Diab. Metab. Res. Rev.* **26**, 287–296 (2010).

53. Williams, D. L., Baskin, D. G. & Schwartz, M. W. Leptin regulation of the anorexic response to glucagon-like peptide-1 receptor stimulation. *Diabetes* **55**, 3387–3393 (2006).

54. Enriori, P. J. *et al.* Diet-induced obesity causes severe but reversible leptin resistance in arcuate melanocortin neurons. *Cell Metab.* **5**, 181–194 (2007).

55. Glaesner, W. *et al.* Engineering and characterization of the long-acting glucagon-like peptide-1 analogue LY2189265, an Fc fusion protein. *Diab. Metab. Res.* **26**, 287–296 (2010).

56. Young, M. A. *et al.* Clinical pharmacology of albiglutide, a GLP-1 receptor agonist. *Postgrad. Med.* **126**, 84–97 (2014).

57. Painter, N. A., Morello, C. M., Singh, R. F. & McBane, S. E. An evidence-based and practical approach to using Bydureon in patients with type 2 diabetes. *J. Am. Board Fam. Med.* **26**, 203–210 (2013).

58. Wang, J., Wang, B. M. & Schwendeman, S. P. Characterization of the initial burst release of a model peptide from poly(D,L-lactide-*co*-glycolide) microspheres. *J. Control. Rel.* **82**, 289–307 (2002).

59. Zou, P. *et al.* Applications of human pharmacokinetic prediction in first-in-human dose estimation. *AAPS J.* **14**, 262–281 (2012).

60. McDaniel, J. R., MacKay, J. A., Quiroz, F. G. & Chilkoti, A. Recursive directional ligation by plasmid reconstruction allows rapid and seamless cloning of oligomeric genes. *Biomacromolecules* **11**, 944–952 (2010).

61. Burcelin, R., Dolci, W. & Thorens, B. Long-lasting antidiabetic effect of a dipeptidyl peptidase IV-resistant analog of glucagon-like peptide-1. *Metab. Clin. Exp.* **48**, 252–258 (1999).

62. de Meester, I., Lambeir, A. M., Proost, P. & Scharpe, S. Dipeptidyl peptidase IV substrates. An update on *in vitro* peptide hydrolysis by human DPPIV. *Adv. Exp. Med. Biol.* **524**, 3–17 (2003).

63. Holst, J. J. The physiology of glucagon-like peptide 1. *Physiol. Rev.* **87**, 1409–1439 (2007).

64. Miranda, L. P. *et al.* Design and synthesis of conformationally constrained glucagon-like peptide-1 derivatives with increased plasma stability and prolonged *in vivo* activity. *J. Med. Chem.* **51**, 2758–2765 (2008).

65. Amiram, M., Luginbuhl, K. M., Li, X., Feinglos, M. N. & Chilkoti, A. Injectable protease-operated depots of glucagon-like peptide-1 provide extended and tunable glucose control. *Proc. Natl Acad. Sci. USA* **110**, 2792–2797 (2013).

66. Meyer, D. E. & Chilkoti, A. Purification of recombinant proteins by fusion with thermally-responsive polypeptides. *Nat. Biotechnol.* **17,** 1112–1115 (1999).

67. Chizzonite, R. *et al.* IL-12: monoclonal antibodies specific for the 40-kDa subunit block receptor binding and biologic activity on activated human lymphoblasts. *J. Immunol.* **147,** 1548–1556 (1991).

68. Goke, R. & Conlon, J. M. Receptors for glucagon-like peptide-1(7-36) amide on rat insulinoma-derived cells. *J. Endocrinol.* **116,** 357–362 (1988).

69. Chan, H. M., Jain, R., Ahren, B., Pacini, G. & D'Argenio, D. Z. Effects of increasing doses of glucagon-like peptide-1 on insulin-releasing phases during intravenous glucose administration in mice. *Am. J. Physiol. Regul. Integr. Comp. Physiol.* **300,** 1126–1133 (2011).

70. Ahren, B., Holst, J. J., Martensson, H. & Balkan, B. Improved glucose tolerance and insulin secretion by inhibition of dipeptidyl peptidase IV in mice. *Eur. J. Pharmacol.* **404,** 239–245 (2000).

71. Luginbuhl, K. M. *et al.* Dataset for: One-week glucose control via zero-order release kinetics from an injectable depot of glucagon-like peptide-1 fused to a thermosensitive biopolymer. *figshare* http://dx.doi.org/10.6084/m9.figshare.4903931 (2017).

Acknowledgements

Author contributions

K.M.L. and A.C. conceived and designed the research. K.M.L., J.L.S., X.L. and B.U. performed the experiments. S.B. provided materials for the imaging study. S.A. helped to plan and organize the non-human primate study. M.F. and D.D. provided expertise in endocrinology for the design of *in vivo* studies. E.M.M. assisted in statistical analysis and interpretation of *in vivo* results. K.M.L. and A.C. analysed the results and wrote the manuscript. J.L.S., E.M.M. and D.D. edited the manuscript.

Additional information

Supplementary information is available for this paper.

Reprints and permissions information is available at www.nature.com/reprints.

Correspondence and requests for materials should be addressed to A.C.

How to cite this article: Luginbuhl, K. M. *et al.* One-week glucose control via zero-order release kinetics from an injectable depot of glucagon-like peptide-1 fused to a thermosensitive biopolymer. *Nat. Biomed. Eng.* **1,** 0078 (2017).

Publisher's note: Springer Nature remains neutral with regard to jurisdictional claims in published maps and institutional affiliations.

Competing interests

A.C. is a scientific advisor and is on the board of directors for PhaseBio Pharmaceuticals, which has licensed the ELP technology for drug delivery applications from Duke University.